隔离病区多消杀机器人作业优化调度与路径规划

Optimal scheduling and path planning of multiple robots for disinfection in isolation areas

刘至理　解天佑

zhililiu624@gmail.com

山东省实验中学

摘　要

本文通过调研、分析疫情期间传染病隔离病区消杀作业的实际需求，提出了一种隔离病区多消杀机器人优化调度与路径规划策略。在综合考虑消杀机器人能源消耗、任务级别、起始点位置等约束条件下，基于经典车辆路径问题（Vehicle Routing Problem，VRP）建立多消杀机器人的优化调度模型，并用遗传算法求解所需机器人的最少数量、最优消杀任务分配与消杀顺序。综合运用 A*与动态窗口算法（Dynamic Window Algorithm，DWA）融合方法，实现隔离病区内消杀机器人的全局路径规划与实时动态避障。为大空间复杂动态环境多机器人协同消杀作业提供了一种行之有效的优化调度策略和动态路径规划算法。

最后，以多个医院隔离病区的真实地图为研究对象，利用 MATLAB 和 Webots 分别进行算法仿真和三维仿真环境模拟实验，仿真和模拟实验结果都验证了新策略的有效性和强适用性。

关键词：多消杀机器人，隔离病区，优化调度，路径规划，实时动态避障

ABSTRACT

In this paper, by investigating and analyzing the actual demand of disinfection tasks in isolation areas during the epidemic, a strategy of optimal scheduling and path planning for multiple disinfection robots in isolation areas is proposed. Based on Vehicle Routing Problem (VRP), the optimal scheduling model of multiple disinfection robots is established through comprehensive consideration of the power consumption of disinfection robots, tasks levels and starting positions. Based on this, genetic algorithm (GA) is used to determine the minimum number of robots required, the assignment of disinfection tasks and the sequence of disinfection. Then, global path planning and real-time dynamic obstacle avoidance are realized by A*-dynamic window algorithm (A*-DWA) for disinfection robots in isolation areas. This provides an effective optimal scheduling strategy and dynamic path planning algorithm for the disinfection of multiple robots in large and complex dynamic environment.

Finally, taking the actual maps of the isolation areas in several hospitals as research objects, numerical simulations and the simulation experiments in three-dimensional physical environment are carried out by MATLAB and Webots, respectively. The simulation results verify the effectiveness and applicability of the proposed strategy.

Key Words: Multiple disinfection robots，isolation areas，optimal scheduling，path palnning, real-time dynamic obstacle avoidance

目 录

1 研究背景与实际需求 **1**

2 多机器人消杀任务问题描述 **3**

3 多消杀机器人优化调度建模与分析 **4**

3.1 多消杀机器人优化调度建模 4

3.2 多消杀机器人优化调度策略 7

4 隔离病区多消杀机器人 A*-DWA 融合路径规划算法 **9**

4.1 多消杀机器人静态全局路径规划算法 9

4.2 多消杀机器人局部动态避障规划算法 12

4.3 基于 A*-DWA 融合算法的多消杀机器人全局动态路径规划 14

5 多消杀机器人系统仿真与验证 **15**

5.1 隔离病区多消杀机器人优化调度策略仿真验证 15

5.2 消杀机器人路径规划与动态避障方法仿真验证 18

5.3 基于 A*-DWA 融合算法的模拟环境全局动态路径规划仿真验证 21

6 结论 **23**

7 参考文献 **24**

8 致谢 **26**

9 附件 **27**

1 研究背景与实际需求

2019 年 12 月突如其来的新型冠状病毒导致的肺炎（简称 COVID-19）疫情爆发，并迅速席卷全球。截至 2021 年 8 月 19 日，造成了 2.1亿人感染和440万人死亡的新冠肺炎已经成为了严重威胁人类安全的全球性流行病[1]。根据权威评估，新冠肺炎的危害将远远超过经济危机和恐怖主义[2,3]。国际社会投入大量资源用于疫情防控，但因感染病例激增，医护资源仍供不应求，特别是医务人员更是日渐短缺。奋战在抗疫一线的医护人员，不仅要承担超负荷的工作，还要面临随时被感染的巨大风险[4]。2020 年 7 月 17 日，世界卫生组织的报告显示，全球新冠确诊病例中医护人员的感染率约为 10%，这就意味着全球医护人员新冠病毒感染病例已超过 140 万例。据不完全统计，截至 2020 年 9 月 2 日，世界上至少已有 7000 名医务人员死于 COVID-19[5]。

COVID-19 具有传播迅速，传染性强，传播途径广等特点，且目前还没有确认有效的治疗方法[6]。但可以确定的是，COVID-19 的主要传播途径为空气传播，对隔离病区消毒杀菌能够有效预防和控制 COVID-19 疫情蔓延。因此，消毒杀菌成为隔离病区中的一项十分重要工作。目前，消杀方法主要有紫外线直接照射法、含氯消毒液喷洒法等方式[7]。传统消杀方式主要是人工消杀，且存在诸多弊端。例如，紫外线消毒设备需要在工作人员撤离后方能照射消毒，而且照射范围有限，会造成消毒不彻底。对于消毒液喷洒方式，由于隔离病区消毒频率高、高浓度含氯消毒液腐蚀性强，导致消毒人员的工作量繁重，安全风险极大。

随着智能机器人技术的发展，机器人系统已在军事、工农业、医疗等领域发挥着越来越重要的作用[8-11]，特别是在医疗领域中，多款医疗服务机器人，如靶向治疗微型机器人[9]，消毒机器人[10]，导诊机器人和室内配送机器人[11]等在疫情防控、疾病诊断中发挥了重要作用。根据中国智能产业联盟的调研报告显示，智能服务机器人是 COVID-19 疫情防控中使用最多的人工智能产品，有效地解决了很多疫情防控难题，如医疗物资配送不及时、消毒任务繁重、医护人员短缺等。消杀机器人是目前应用广泛的病区智能服务机器人[12]，具有高机动、低能耗、高容错等优势，能够在 COVID-19 消毒杀菌环节中减轻医护人员的繁重工作量，

并且减少医护人员感染几率。同时，与人工操作相比，机器人凭借智能化、可控性等优势，能够有效提高消毒杀菌工作的效率[13]。因此，深入研究消毒杀菌机器人及其优化作业对 COVID-19 疫情防控意义重大。

近年来，智能化自主消毒杀菌装备已被用于医学临床一线。2012 年，Shatalov 等[14]设计了一种能有效杀菌消毒的紫外线发射装置。随后，分别验证了使用便携式紫外线设备和在机器人上搭载便携设备进行消毒的可行性[15,16]。2015 年，美国谢尼克斯消毒服务公司生产的一种紫外线辅助消毒机器人被用于抗击埃博拉疫情的一线，它通过发射氙气产生紫外线脉冲来杀灭病原体，以有效保护医护人员。此外，Chanprakon 开发了一种具有自主避障功能的紫外线机器人，实现手术室或病房 360°全方位消毒[17]。

在我国此次抗击 COVID-19 疫情过程中，部分国产智能机器人产品已在现场应用，特别是消杀类机器人。如上海钛米机器人科技有限公司研发的消毒机器人，集成过氧化氢、紫外线、等离子空气过滤等多种方式对多重场景消毒[18]。上海梵通生物科技有限公司研制的消毒机器人，结合过氧化氢高水平消毒技术和人工智能技术，实现医院病房、手术室等的消毒杀菌。湖南大学国家重点实验室及湖南爱米家智能科技公司等合作研制的医用紫外线消毒机器人，能以紫外线照射和消毒液喷洒两种形式对医院病房进行消毒，并且具备智能自主导航功能[19]。杭州电子科技大学研发的强紫外线杀菌机器人通过自动规划路径、自主移动实现高效的紫外线杀菌[20]。大陆智源科技有限公司研发的消杀机器人，以次氯酸钠作为主要消毒剂，可根据消杀区域面积、人员数量等环境信息，自主设置消杀浓度、喷洒模式等参数，已在武汉协和医院、黄冈市中心医院、黄冈妇幼保健院等抗疫一线成功应用。

尽管消杀机器人已在部分现场应用，但从我们刚刚完成的调研情况来看：**现有的机器人尚不能有效解决隔离病区消杀中普遍存在的智能水平低、应变能力差等问题。主要表现在：作业模式以单机作业、固定路径为主，难以应对大型复杂场景多机协同作业任务，特别是对于具有时间约束的每日多频次的实际消杀作业需求，以及对作业环境中动态障碍物实时规避缺乏有效解决方案。**

本文在新冠肺炎疫情迅速传播的急切形势下，针对 COVID-19 抗疫机器人消

杀模式单一、能耗大、消杀时间长等实际难题，综合考虑消杀机器人动力电池剩余电量、重点区域消杀任务、初始位置等约束条件，基于 VRP 模型提出隔离病区多消杀机器人多约束条件优化调度策略。针对隔离病区环境的特殊性，提出多机器人路径规划 A*和 DWA 融合算法，实现既定环境下全局路径规划与未知环境的局部实时动态避障。结合武汉火神山医院、武汉大学人民医院隔离病区地图的实际数据，搭建三维仿真环境，分别开展多消杀机器人的全局路径规划、动态实时路径规划和跟踪实验，以验证所提控制方法的可行性和有效性。

2 多机器人消杀任务问题描述

本文主要研究隔离病区中多消杀机器人的优化调度与路径规划问题，整体框架如图 1 所示。每个消杀机器人从充电站出发，完成分配的消杀任务后返回。按照医院的消杀标准，单次消杀任务应在限定时间内完成。在机器人的负载、剩余电量和重点区域消杀任务等约束下，设计优化调度策略以确保任务中所需机器人最少，移动路径最短，并确定每个机器人的消杀病房顺序。

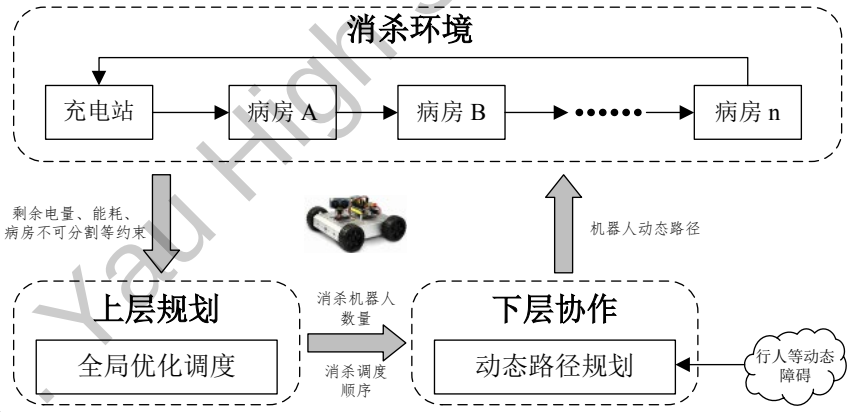

图 1 消杀机器人优化调度与路径规划示意图

假设已知病房位置、病房消杀量、机器人行走速度、单位距离耗电量、充电站的位置。此外，假设在一个消杀周期内，每个病房只被一个机器人消杀一次。因此，可以将多机器人在隔离病区内的消杀作业归结为一个典型的带有多约束的任务优化问题和大型复杂环境下的路径规划问题。基于隔离病区多机器人消杀任务需求，提出多机器人在能耗、病区环境和消杀任务等约束下的优化调度策略。

藉此，基于 A*和 DWA 融合算法，提出一种新颖的路径规划策略，实现多机器人消杀全局最优动态避障。

3 多消杀机器人优化调度建模与分析

本节主要针对多消杀机器人的最优调度问题进行建模和分析。具体而言，首先基于 VRP 建立具有多个约束条件的多消杀机器人优化调度模型，然后采用遗传算法求解最优调度问题。

3.1 多消杀机器人优化调度建模

基于 VRP 模型[21]，对隔离病区带约束的多消杀机器人优化调度问题建模，该优化调度问题的宗旨是求解隔离病区内所需消杀机器人的最少数量和消杀调度顺序，即在规定时间内使用尽可能少的机器人完成消杀任务且总路径最短。

具体而言，利用图论将病区消杀问题描述为：在一个无向图$G=(V,E)$，其中$V=\{0,1,...,n\}$表示病区内所有节点集合，0 表示充电站节点，$\{1,...,n\}=:V'$为病房节点集合，$E=\{(i,j)|i,j\in V,i\neq j\}$表示边集，每条边的权重为$c_{ij}\left(i,j\in V,i\neq j\right)$表示从节点$i$到节点$j$的最短路径，且有如下假设：

需求量：

每个病房i所需的消杀量d_i是固定的，且护士站配有足够的消毒用品。

多机器人：

可提供消杀的机器人集合为$K=\{1,...,m\}$，每台机器人型号相同，容量相同均为Q，且每台机器人的剩余电量分别为P_k，$k=1,...,m$。

约束条件：

① 机器人均始于充电站，完成所分配的消杀链上所有任务后最终返回充电站。

② 在一个消杀周期内每个病房的消杀任务只能由一台机器人完成。

③ 完成任务链上病房消杀任务所需消毒液总量必须小于等于机器人容量且每一条消杀任务链上至少有一个病房点。

④ 机器人完成消杀任务所需电量要小于等于机器人电量。

⑤ 每一条消杀任务链上的消杀任务均在规定时间内完成。

该优化调度问题中所涉及的参数及相关变量如表 1 和表 2 所示：

表 1 集合含义

集合	含义
$V=\{0,1,...,n\}$	病区内所有节点集合（0 表示充电站节点）
$V^{'}=\{1,...,n\}$	病房节点集合
$K=\{1,...,m\}$	消杀机器人集合
S_k	为机器人 k 所分配任务链上的病房节点集合

表 2 参数含义

参数	含义
c_{ij}	边的权重，表示从节点 i 到节点 j 的最短路径 $(i,j\in V,i\neq j)$
Q	机器人容量（最大负载量）
d_i	病房 i 的消杀需求量
P_k	机器人 k 的剩余电量
λ_1	机器人移动单位距离所消耗的电量
λ_2	机器人消杀单个病房所消耗的电量
t_1	机器人移动单位距离所需的时间
t_2	机器人消杀单个病房所需的时间
T	机器人完成病区消杀任务的规定时间

决策变量：

$$x_{ijk}=\begin{cases}1,\text{机器人}k\text{从节点}i\text{移动到节点}j,\\0,\text{其他。}\end{cases} \tag{1}$$

目标函数：

$$\min F=\sum_{k\in K}\sum_{i\in V}\sum_{j\in V}c_{ij}x_{ijk} \tag{2}$$

s.t.

$$\sum_{i\in V}x_{0ik}=1,k\in K, \tag{3}$$

$$\sum_{i\in V}x_{ilk}=\sum_{j\in V}x_{ljk},l\in V,k\in K, \tag{4}$$

$$\sum_{j\in V}x_{j0k}=1,k\in K, \tag{5}$$

$$\sum_{k\in K}\sum_{i\in V}x_{ijk}=1,j\in V', \tag{6}$$

$$\sum_{k\in K}\sum_{j\in V}x_{ijk}=1,i\in V', \tag{7}$$

$$\sum_{i\in S_k}\sum_{j\in S_k}x_{ijk}d_i\le Q,k\in K, \tag{8}$$

$$\sum_{i\in S_k}\sum_{j\in S_k}\lambda_1 c_{ij}x_{ijk}+\lambda_2\left|S_k\right|\le P_k,k\in K, \tag{9}$$

$$\sum_{i\in S_k}\sum_{j\in S_k}x_{ijk}\le\left|S_k\right|-1,k\in K, \tag{10}$$

$$\sum_{i\in S_k}\sum_{j\in S_k}t_1 c_{ij}x_{ijk}+t_2\left|S_k\right|\le T,k\in K, \tag{11}$$

$$x_{ijk}\in\{0,1\},i,j\in V,k\in K. \tag{12}$$

式(3)-(5)表示每个机器人从充电站出发，任务链上前一个病房节点消杀完毕后会转移至下一个病房节点消杀，完成任务链上所有消杀任务后，最终返回至充电站。式(6)-(7)表示同一消杀周期内每个病房只被一台机器人消杀一次。不等式(8)表示每一条任务链上的病房消杀总需求量不能超过机器人的最大负载量。不等式(9)表示机器人完成任务链上的消杀任务所消耗电量小于等于机器人的剩余电量。不等式(10)为支路消除约束。不等式(11)表示机器人完成任务链上消杀任

务所需总时间不超过规定时间。式(12)为决策变量属性。

3.2 多消杀机器人优化调度策略

常用的优化调度算法有：蚁群算法[22]，遗传算法[23]等。蚁群算法是一种贪婪启发式算法，存在收敛速度慢、易陷入局部最优解等缺点。遗传算法能够有效地在概率意义下全局搜索，具有内在的并行性和更好的全局寻优能力，能自动获取和指导优化的搜索空间，自适应地调整搜索方向。针对上节所建模型，本节采用遗传算法求解优化调度问题。求解步骤如下。

编码方案设计：

VRP 为一个离散优化问题，结合约束条件式(6)-(7)对病房采用自然数编码[24,25]，即 0 表示充电站节点，1,…,n 为病房节点，如需消杀机器人数量为k，则染色体长度为$n+k+1$。

种群初始化：

首先将所有病房代码随机排成一列，q_i 代表染色体中第i个病房消耗电量。如果$\sum_{i=1}^{a} q_i \le Q$且$\sum_{i=1}^{a+1} q_i > Q$，则在染色体第a位后面插入 0；然后从插入 0 后开始重复计算直至代码列最后；随后将染色体的首位及最后一位分别插入一个 0，最终形成一条初始染色体；重复上述过程产生由 N 条个体构成初始种群，其中 N 为初始种群数。

约束处理与适应度函数：

在满足约束条件式(3)-(5)及(8)-(9)的前提下，将染色体解码为机器人的消杀路径。根据消杀序列路径，当机器人到达第一个病房并完成消杀后，判断该机器人的最大剩余电量是否能够保证机器人返回充电站。再确定如果将第二个病房加入第 1 台机器人的路径是否满足以上条件。如果满足，则第 1 台机器人的行驶路线为 0-1-2-0。依次类推，一旦上述条件不能满足，则需要增加 1 台机器人，即规划从充电站出发的第 2 条行驶路线。

根据解码出来的机器人消杀路径，计算式(2)所示的目标函数，由于适应度

函数要求越大越好，因此我们将设计的目标函数的倒数作为适应度函数，即适应度函数为：

$$fit(i)=\frac{1}{\sum_{k\in K}\sum_{i\in V}\sum_{j\in V}c_{ij}x_{ijk}}. \tag{13}$$

此外，还需判断机器人行驶路径所耗电量是否超过总剩余电量，若超过，则该消杀路径不可行，该解称为不可行解。通过惩罚函数增大目标值，从而淘汰不可行解。

遗传操作：

（1）选择复制

采用轮盘赌选择，以父代最优染色体替换子代最差染色体。首先计算当前种群中每个染色体的适应度 $fit(i)$，然后计算当前种群中所有染色体适应度的总和：

$$sum\ fit(i)=\sum_{i}^{n}fit(i). \tag{14}$$

其次计算当前种群中各个染色体的选择概率：

$$p(i)=\frac{fit(i)}{sum\ fit(i)},i\in N. \tag{15}$$

最后计算当前种群中各条染色体的累计概率：

$$ps(i)=\sum_{i\in N}p(i). \tag{16}$$

随机产生一个在[0,1]区域内的实数 r，如果满足条件 $ps(i)>r$，则选择使该条件成立的第一条染色体，否则选择使得 $ps(i-1)<r<ps(i)$ 成立的第 i 条染色体。

（2）交叉

首先分别在两个父代染色体 1，2 上随机选择一段子路径 A，B；然后将被选择的子路径前置，随后将父代染色体 1 的子路径 A 作为子代染色体 1 的一部分，同时将父代染色体 2 中子路径 A 没有的编码按照父代染色体 2 中的顺序添加到子路径 A 的后面，在染色体的末尾添加编码 0；最后针对子代染色体 1，在子路径 A 后面多次随机打断，分别计算所有情况的适应度，把适应度值最大的作

为子代染色体 1；同理得到子代染色体 2。

（3）变异

选择 3-交换变异算子使染色体变异，即在父代染色体中随机选择 3 个位置交换，得到 5 个子代染色体，对所有情况计算适应度，适应度最高的进入子代种群。

终止条件：

遗传算法是一种随机搜索算法，为了结束遗传算法的进化循环，必须预先设定终止规则。常见的终止规则有 3 种：一是达到预先设定的目标；二是在连续若干代后，种群中的最优个体没有获得新的改进；三是达到预先设定的进化代数。预先设定进化代数能够有效的控制算法的求解精度和运行时间，因此本文采用事先确定的进化代数作为终止规则。

4 隔离病区多消杀机器人 A*-DWA 融合路径规划算法

路径规划是机器人高效自主运行的前提，可使机器人在复杂环境中沿着最优路径完成工作。根据不同的已知信息量，将路径规划分为静态全局路径规划和局部动态避障路径规划。静态全局路径规划是通过建立全局地图模型寻找一条从起点到终点的最优路径；局部动态避障路径规划则是根据机器人当前所处的局部环境，通过传感器检测周围环境，具有更强的实时应变能力和避障能力。因此，综合考虑静态全局路径规划策略与局部动态避障路径规划策略，具有重要的理论价值和现实意义。

4.1 多消杀机器人静态全局路径规划算法

在实际执行任务的过程中需要通过静态全局路径规划来保证消杀机器人从初始位置到目标位置的行进路径最短。常见的静态全局路径规划算法有基于采样的规划算法和基于图的搜索算法。其中基于采样的规划算法包括随机路径图法（Probabilistic Roadmaps，PRM）和快速探索随机树（Rapidly-exploring Random Trees，RRT）等，基于图的搜索算法包括 Dijkstra 算法（D 算法）和 A*算法等。PRM 算法的求解精度与其选取的节点数有关，当节点数较多时，PRM 也可求得

最优解，但无疑会增加计算量，降低效率[26]。RRT 算法是一种适用于多维空间的路径规划方法，通过对空间中的路点随机采样寻找路径，但该方法所求得的路径往往不是最优的[27]。D 算法从起始点延伸到外层直到终点，但是 D 算法采取的盲目搜索策略，在搜索过程中包含了很多无意义的点，从而导致时间复杂度很高，计算效率低[28]。A*算法是一种经典启发式搜索算法[29]，通过一次扩展具有最小启发函数的节点来求解静态环境中最短路径，并且能够保证找到全局最优解，相对于 D 算法，A*算法大大提高了搜索效率。因此，本文选用 A*算法寻找消杀机器人的期望路径。

A*算法原理：

首先将路径搜索空间划分为栅格形式，通过比较当前位置的 8 个相邻栅格代价函数来逐步确定下一路径位置，搜索过程如图 2 所示。蓝色圆圈代表当前位置节点，数字 1-8 代表当前位置的 8 个相邻节点。在图 2 中，蓝色箭头代表当前位置到下一位置的一种选择。

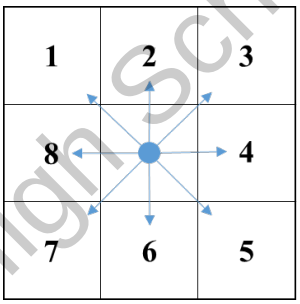

图 2 传统 A*算法搜索过程

算法流程：

A*算法的流程由如下图 3 所示，具体地：

（1）初始化相关参数，生成 open list 和 close list，设置搜索空间范围。

（2）已知 open list 判断是否包含目标位置，若包含，则结束路径规划；否则执行下一步。

（3）计算 open list 中各节点的代价函数，找出其中的最小值所对应节点，并将该节点设为当前节点，同时将该节点加入 close list，代价函数表达式如下：

$$F(n)=g(n)+h(n), \tag{17}$$

其中，n 为当前节点；$g(n)$ 为从路径的起始位置到当前节点的实际代价值；$h(n)$

为从当前节点到路径目标位置的估计代价值（即启发函数）。

（4）对当前节点周围的 8 个相邻节点分析计算。

① 若该点为障碍物或在 close list 中，则该点不予考虑。否则，进行下一步操作。

② 若该点不在 open list 中，将该点加入 open list 中，并将当前节点设为该点父节点，记录该点代价函数。

③ 若该点在 open list 中，检查移动到该点是否为最优路径点（用 $g(n)$ 来判断， $g(n)$ 越小路径越优）；如果是最优路径点则保留该点同时将该节点的父节点设为当前节点，并重新计算该点代价函数。

（5）返回步骤（2）。

其中，open list 记录所有可能会经过的位置点，close list 记录移动对象经过的每个位置点。

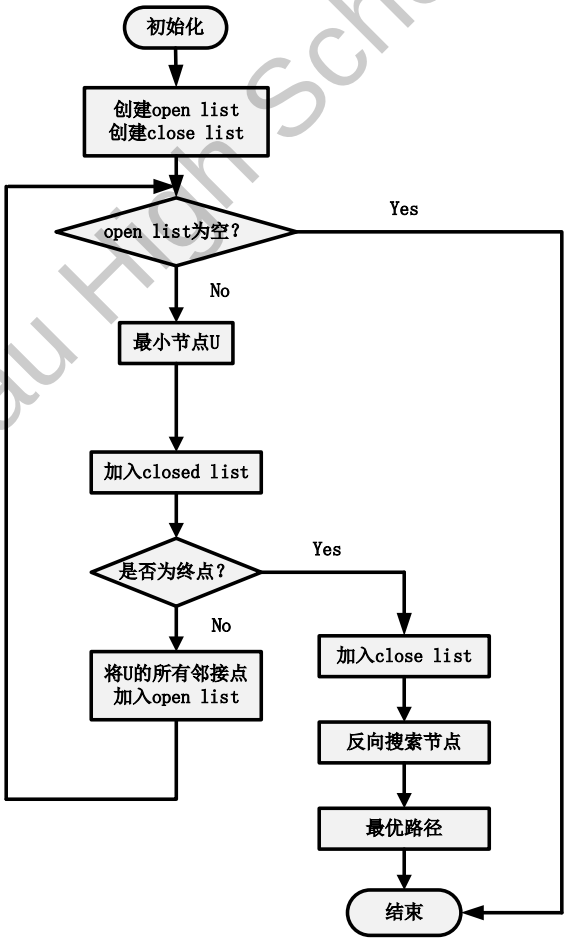

图 3　A*算法流程图

4.2 多消杀机器人局部动态避障规划算法

在实际的隔离病区，不可避免地存在来往的医护人员、临时堆放的物品等动态障碍物，因此，消杀机器人应能动态避障。常用的动态避障算法有人工势场法[30]，DWA[31]，模糊控制[32]及神经网络[33]等。人工势场法具有算法简洁易懂等特点被广泛应用于路径规划中，但其算法中引力场与斥力场的选取容易使得机器人陷入局部最优点导致机器人崩溃。DWA 是一种常用的动态避障算法，它是在指令区域内搜索出最优控制指令，以使目标函数组最大化。通过在速度空间中采样多组速度，并在这些速度下模拟机器人在一定时间内的轨迹，利用离散小波分析可以得到多组运动轨迹。然后，通过评估这些轨迹找到最优轨迹，并采用该最优轨迹相对应的速度来驱动机器人，最终实现动态避障。DWA 是根据自身传感器实时完成环境监测，选取合适的前进策略，其算法计算量小，实时性高，并且可以和其他路径规划算法融合使用。

本文选用 DWA 算法来实现局部动态避障。在二维平面下，机器人位置可以转换成为速度、角速度的函数。

在连续情况下：

$$x(t_n) = x(t_0) + \int_{t_0}^{t_n} v(t)\cos\theta(t)dt, \tag{18}$$

$$y(t_n) = y(t_0) + \int_{t_0}^{t_n} v(t)\sin\theta(t)dt, \tag{19}$$

$$\theta(t_n) = \theta(t_0) + \int_{t_0}^{t_n} \omega(t)dt, \tag{20}$$

其中 $v(t)$ 是线速度； $\theta(t)$ 是方向角； $\omega(t)$ 是角速度。

在离散情况下：

$$\Delta x = v_x \Delta t\cos\theta_t - v_y \Delta t\sin\theta_t, \tag{21}$$

$$\Delta y = v_x \Delta t\sin\theta_t + v_y \Delta t\cos\theta_t, \tag{22}$$

$$\Delta\theta_t = \omega_t \Delta t, \tag{23}$$

其中 v_x 和 v_y 分别是线速度沿 x 轴和 y 轴的分量； θ_t 是方向角； ω_t 是角速度。

约束条件：

① 机器人最大、最小速度约束

使得机器人速度约束满足机器人线速度、角速度要求。

$$V_m = \{(v,\omega) \mid v \in [v_{\min}, v_{\max}] \wedge \omega \in [\omega_{\min}, \omega_{\max}]\}, \tag{24}$$

其中 $v_{\min}$ 和 $v_{\max}$ 分别是机器人最小和最大线速度； $\omega_{\min}$ 和 $\omega_{\max}$ 分别是是机器人最小和最大角速度；

② 加减速约束

机器人在前进时间段内，动态窗口 V_d 定义为：

$$V_d = \{(v,\omega) \mid v \in [v_c - \dot{v}\Delta t, v_c + \dot{v}\Delta t] \wedge \omega \in [\omega_c - \dot{\omega}\Delta t, \omega_c + \dot{\omega}\Delta t]\}, \tag{25}$$

其中 v_c 和 ω_c 分别是机器人当前线速度和角速度；$\dot{v}$ 和 $\dot{\omega}$ 分别是机器人的加速度和角加速度； Δt 为加速度 $\dot{v}$ 和角加速度 $\dot{\omega}$ 作用的时间。

③ 制动距离约束

为保证机器人安全，在最大减速度条件下，机器人在当前速度应能在撞击障碍物之前减速为 0。

$$V_a = \{(v,\omega) \mid v \le (2dist(v,\omega)\dot{v}_b)^{\frac{1}{2}}, \omega \le (2dist(v,\omega)\dot{\omega}_b)^{\frac{1}{2}}\}, \tag{26}$$

其中 $dist(v,\omega)$ 为轨迹上到障碍物的最近距离。

评价函数：

由于若干组采样速度在速度空间内是可行的，因此，需通过设计合理的评价函数用来选取最优轨迹。评价函数的设计准则为：保证机器人在避开障碍物的前提下朝向目标快速前进。根据此准则设计的评价函数为：

$$G(v,\omega) = \sigma(\alpha head(v,\omega) + \beta dist(v,\omega) + \gamma vel(v,\omega)), \tag{27}$$

其中 $\sigma(\cdot)$ 为平滑函数， $head(v,\omega)$ 为方位角评价函数，表示在当前速度下，机器人当前目标位置与终点位置的方位角偏差； $vel(v,\omega)$ 为当前速度的评价函数；

α, β, γ 为加权系数。

4.3 基于 A*-DWA 融合算法的多消杀机器人全局动态路径规划

虽然 A*算法是最有效的静态全局路径规划算法，但不能应对随时出现的动态障碍物。而 DWA 算法具有良好的动态避障能力，但又因没有考虑静态全局路径最优的要求，存在容易陷入局部最优致命性缺陷。因此，本文提出融合 A*与 DWA 的动态路径规划算法，保证了动态规划路径的全局最优性，算法流程如图 4 所示。

将公式(27)中的 $head(v,\omega)$ 函数转换为 $PHead(v,\omega)$，其中 $PHead(v,\omega)$ 为机器人当前目标位置与终点位置的方位角偏差，当前目标位置是全局最优路径上距离机器人当前位置最近的序列点，则评价函数变为：

$$G(v,\omega)=\sigma(\alpha PHead(v,\omega)+\beta dist(v,\omega)+\gamma vel(v,\omega)). \tag{28}$$

该评价函数既能保证局部路径规划遵循全局最优路径，又能使机器人沿着全局最优路径实现动态避障。

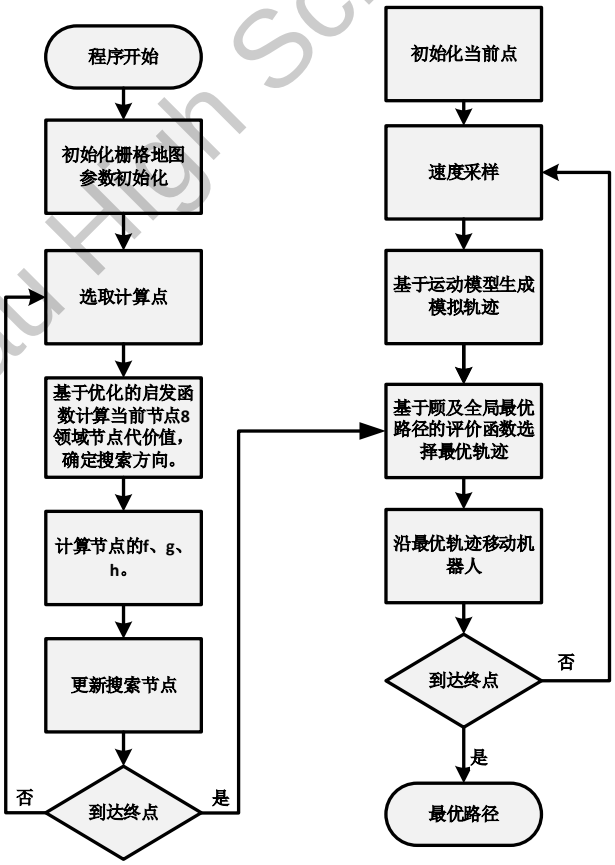

图 4 A*-DWA 算法搜索过程

5 多消杀机器人系统仿真与验证

这里参照武汉火神山医院和武汉大学人民医院的隔离病区平面图，设计了简化的仿真地图，如图 5 所示。病区内每个病房的进深为 3m，开间为 2.2m，病区走廊宽 1.5m，大厅走廊宽 6.4m，基于上述数据设计仿真实验环境。

结合隔离病区的消杀任务需求，采用 MATLAB 与 Webots+Python 对所提出新算法进行仿真与模拟实验。值得说明的是：以下所有实验均在 16GB RAM，Intel Core™ i5-8265U CPU 和 1000G 硬盘的电脑上完成。

(a) 火神山医院平面图

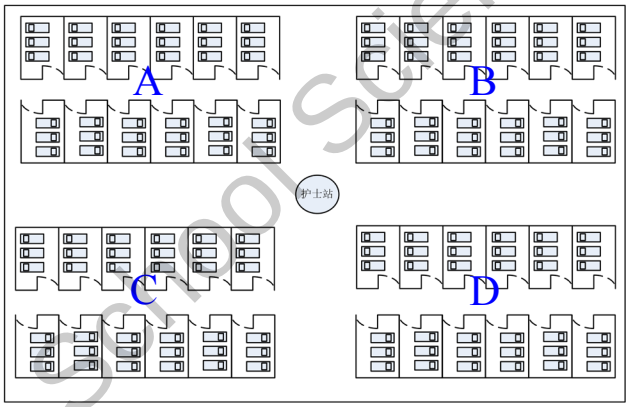

(b) 火神山医院部分参考设计图

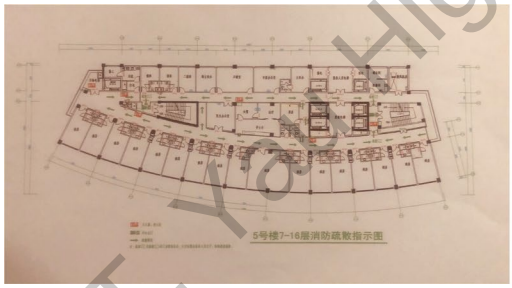

(c) 武汉大学人民医院某病区平面图

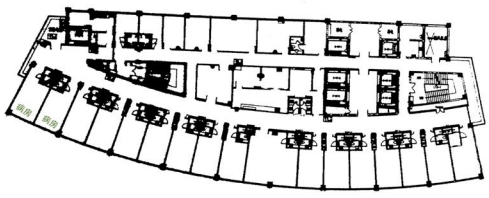

(d) 武汉大学人民医院某病区参考设计图

图 5 隔离病区设计图

5.1 隔离病区多消杀机器人优化调度策略仿真验证

在本实验中，综合考虑各机器人剩余电量、重点区域消杀任务、不同初始位置等条件，基于遗传算法求解多消杀机器人的优化调度策略。假设算法均采用自然数编码方式，初始种群大小即 NIND 为 100，最大迭代次数为 200，交叉概率

为 0.9，变异概率为 0.1。截取的火神山隔离病区由 A、B、C、D 四个单元病区组成，每个病区拥有 12 间结构相同病房。图 6 中，位于中心位置的黑色汇聚点表示机器人的出发点与结束点（即充电站所在位置），其他每个节点分别表示不同病房的中心位置。封闭图代表算法在约束条件下规划出的机器人最优调度策略，其中不同颜色的封闭图分别对应不同机器人的病房消杀路线。

实验（1）：假设每个消杀机器人均配备动力锂电池，其中消杀每个病房耗电量一定，电耗为 1Ah，机器人行走距离与耗电量呈线性关系，比例为 1：1。在机器人剩余电量分别为 20Ah、40Ah、60Ah 时，基于遗传算法完成了机器人的数量选择与优化调度。在消杀任务相同但机器人初始电量不同情况下的优化调度如图 6 所示。可以看出，求解出的最优机器人数分别为 7 台、4 台、4 台。

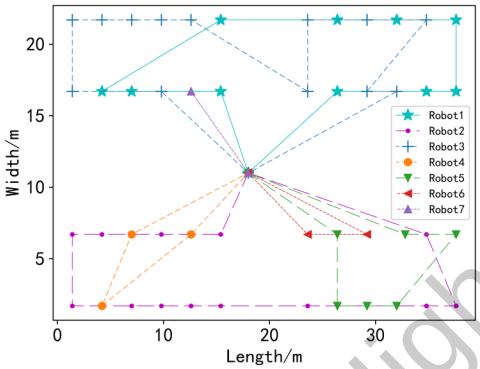

(a) 机器人剩余电量为 20Ah 任务分配情况

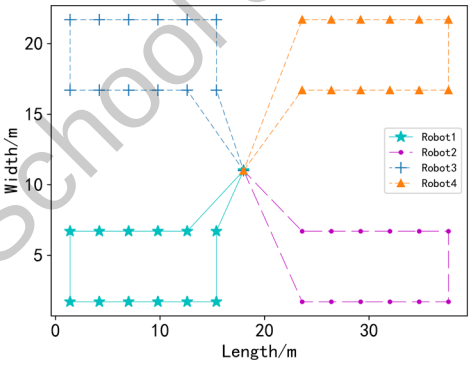

(b) 机器人剩余电量为 40Ah 任务分配情况

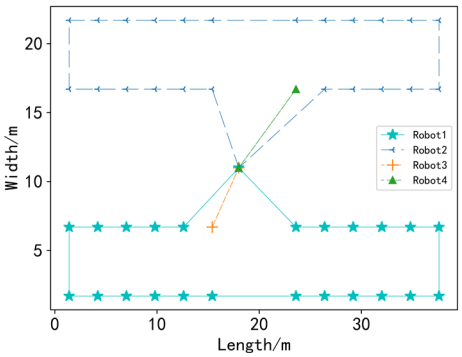

(c) 机器人剩余电量为 60Ah 任务分配情况

图 6 不同剩余电量下的优化调度

消杀机器人优化调度迭代过程如图 7 所示，每代中最优目标值函数即为调度规划路线总距离，其中蓝线表示每代中的最小目标函数值，红线表示每代种群平

均目标函数值。显而易见，随着迭代次数的增多，目标函数数组明显减小，并最终收敛。

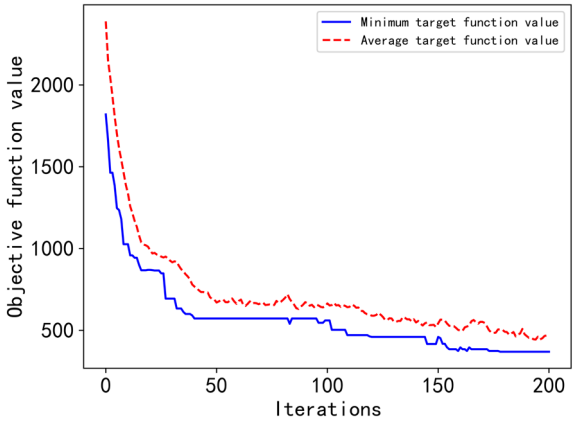

图 7 消杀机器人调度优化迭代过程

实验（2）：在机器人剩余电量为 40Ah 时，假设需要对隔离单元 A 的 9 个病房和隔离单元 C 的 6 个病房进行重点消杀，即消杀 A，C 单元中每个病房所消耗的电量增加一倍。在相同机器人初始电量，但消杀任务不同情况下的优化调度如图 8 所示。从图中可以看出，相比于图 6(b)，机器人重新进行了调度策略的优化。

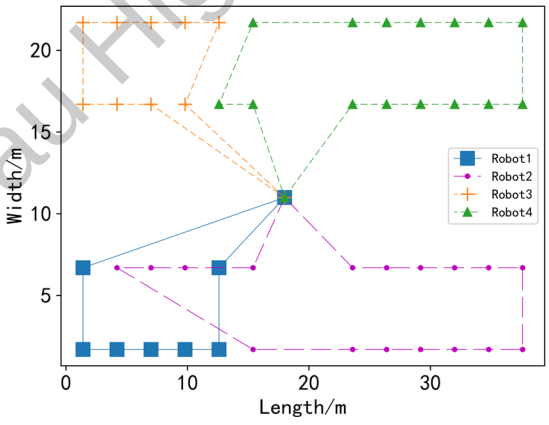

图 8 重点消杀病房的任务分配情况

实验（3）：考虑不同医院隔离病区的实际情况不同，机器人初始位置设置也不尽相同。因此假设当机器人初始位置即充电站位置改变，如将两个充电站各自设置在隔离病区 A、B 单元之间以及 C、D 单元之间，重新调度分配存储电量为 20Ah 的机器人的任务，其任务调度分配情况如图 9 所示。可以看出调度算法

均采用就近原则来确保适应度函数值最优。

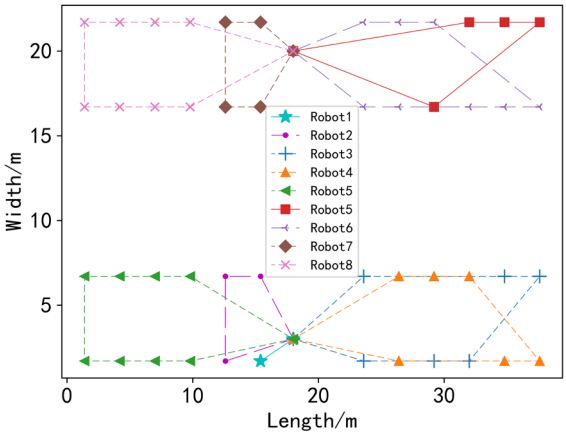

图 9 充电站位于南北消杀单元的任务分配情况

5.2 消杀机器人路径规划与动态避障方法仿真验证

实验（1）：在全局地图已知情况下，本实验采用 A*算法实现单个消杀机器人全局最优路径规划，且与采用 RRT 算法的情形对比。实验设置为：机器人的大小为 0.4*0.4 m^2，运行速度为 1m/s，转弯半径 1.5m。采样时间 T=0.1s。

（1）在图 5（b）所示的地图中，假设机器人初始状态为：Xstart=[19，11，0]，Ygoal=[31，16，0]，全局搜索范围：38*22 m^2。

（2）在图 5（d）所示的地图中，假设机器人初始状态为：Xstart=[270，120，0]，Ygoal=[90，110，0]，全局搜索范围：500*200 m^2。

基于 A*算法规划的全局最优路径如图 10 中红色曲线所示，其中绿点表示机器人的起点，红点表示预设的机器人目标位置。图 10(a)为采用 A*算法分别在两个地图上得到的全局路径规划，由图可以看出，A*算法规划出的最优路径平滑且无碰撞。图 10(b)为 RRT 算法规划的全局路径，由图可知，RRT 算法首先进行全局随机路点的遍历，然后选取最优路径，因此算法的计算量大，得到路径轨迹并非最优且不平滑。

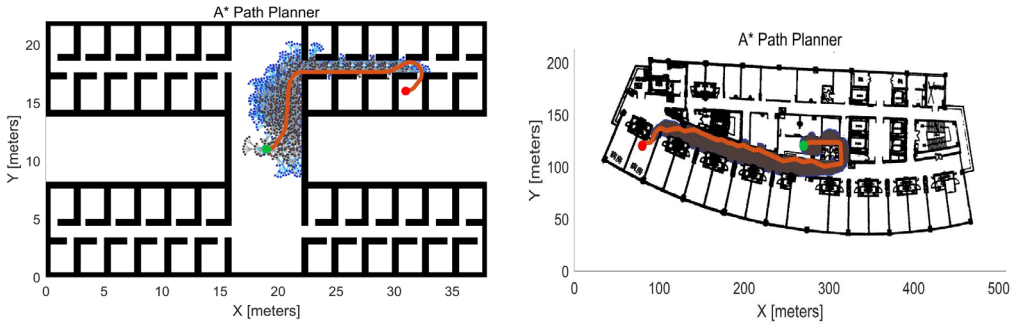

(a) A*算法规划最优路径

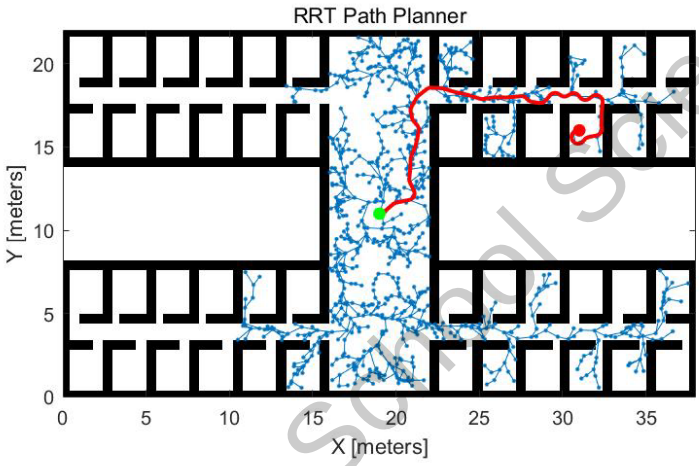

(b) RRT 算法规划的路径

图 10 单个消杀机器人路径规划

实验（2）：本实验中，针对图 5（b）所示地图，采用 A*算法实现两台消杀机器人的最优路径规划。本实验中，假设两个机器人的初始状态分别为：

机器人 A：起始点 1：Xstart1=[19，11，0]，目标点 1：Ygoal1=[31，16，0]。

机器人 B：起始点 2：Xstart2=[19，10，0]，目标点 2：Ygoal2=[13，2，0]。

仿真参数为：机器人的大小为 0.4*0.4 m^2，运行速度为 1m/s，转弯半径 1.5m，采样时间 T=0.1s，全局搜索范围：38*22 m^2。当两台机器人的目标位置不同时，其最优路径如图 11 所示。由图可以看出，A*算法实现了不同初始位置和目标位置下两台机器人的全局无碰撞最优路径规划。

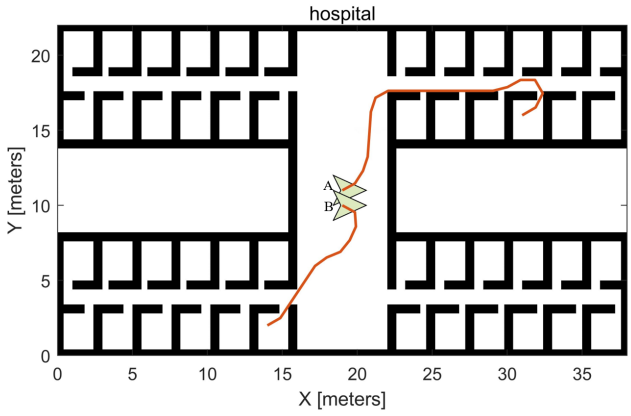

图 11 A*算法规划两台消杀机器人的路径

实验（3）：本实验验证了 A*算法的动态避障效果。实验设置了两个在机器人运行 1 秒后出现的障碍物，规划的路径如图 12(a)所示。其中蓝色与黄色区域分别表示消杀机器人 A、B 的距离传感器可达的视野范围，颜色越深表示可视范围越近。从图中可以看出，两台消杀机器人分别遇到一个障碍物时，机器人 A 进行 3 次路径规划，而机器人 B 进行 4 次路径规划。

假设机器人 A 在完成一次避障后，其行走路径上突然出现第二个障碍，此时机器人会再次进行路径规划以规避障碍，如图 12(b)所示。此时机器人 A 从初始点到目标点共进行了 5 次路径规划。

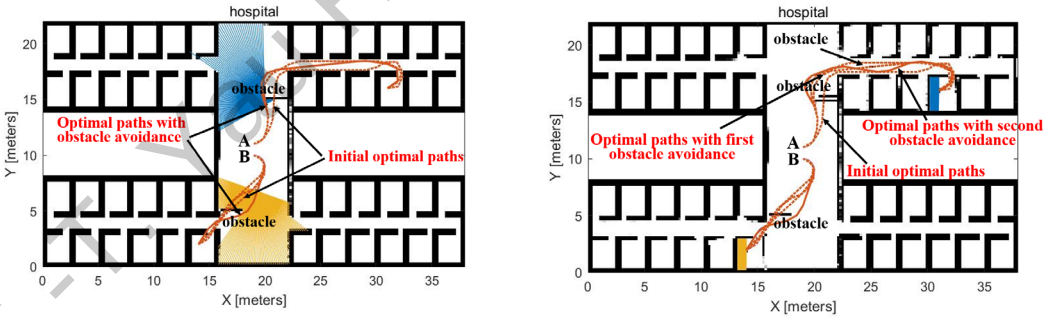

(a) A*算法规划消杀机器人一次避障　　(b) A*算法规划消杀机器人二次避障

图 12　A*算法的避障轨迹规划

由上述仿真实验可知， A*算法可以有效地实现基于已知地图的全局路径规划，但在遇到动态障碍物时，机器人需重新规划全局路径以避免与障碍物的碰撞，实时性较差。

5.3 基于 A*-DWA 融合算法的模拟环境全局动态路径规划仿真验证

由于导航使用的传感器等物理元器件在 MATLAB 仿真中较为繁琐，因此，以下实验均用三维物理仿真平台 Webots+Python。Webots 是一个开源的物理仿真环境，具有接近实际的物理仿真元件与丰富的传感器种类。

本三维物理环境仿真实验分别基于武汉火神山医院和武汉大学人民医院的隔离病区简化地图。首先构建了火神山医院部分隔离区病房的物理模型，如图 13（a）所示。在火神山医院的设计图中，消杀机器人的起点位于隔离病区中央的充电站。即图中灰色柱体为充电站，4 个青色方块为 4 台消杀机器人。整个仿真模型包含 16 个病房，分别位于地图的四个角，各个病房之间使用墙体进行隔离。武汉大学人民医院的物理模型如图 13（b）所示，隔离病区为不规则结构体，其他与火神山医院相同。

（a）火神山医院部分隔离区简化物理模型（b）武汉大学人民医院部分隔离区简化物理模型

图 13 医院隔离区病房仿真模型图

实验（1）：本实验验证无动态障碍物时的路径规划与跟踪。假设消杀机器人的剩余电量为 40Ah，采用 A*算法规划机器人的消杀路径，如图 14 所示。机器人按调度任务链完成各个病房的消杀任务，运动轨迹分别采用不同的颜色表示。

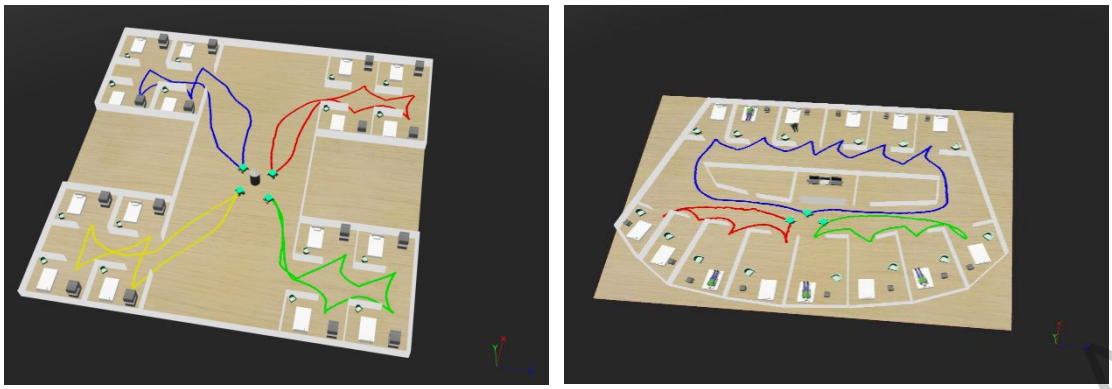

图 14 机器人进行消杀任务的行走路径

实验（2）：本实验验证当环境中出现动态障碍物时，融合 A*与 DWA 算法的动态避障效果，如图 15 所示。由图可以看出，在返程过程中出现动态障碍物（假人）时，机器人能够使用自带的激光传感器进行障碍物检测，完成动态避障，效果如图 15(b)所示。

(a) A*融合 DWA 算法实现动态避障　　(b) 动态避障局部放大图

图 15 A*-DWA 规划的动态避障路径

6 结论

本文通过分析 COVID-19 疫情期间多个医院隔离病区消杀作业实际调研数据，凝练出隔离病区日消杀工作一般性标准与作业需求，结合医用消杀作业有关国家标准的要求，在考虑各消杀机器人剩余电量、重点区域消杀任务、初始位置等约束条件，基于 VRP 模型提出了隔离病区多消杀机器人多约束条件优化调度策略，实现了不同任务需求下的多消杀机器人的优化调度；针对隔离病区环境的动态复杂特性，提出基于 A*和 DWA 融合控制算法的多机器人路径规划，实现了已知环境的全局路径规划与未知环境的局部实时动态避障。通过多约束优化调度策略与 A*和 DWA 融合控制算法相结合，有效地解决了大空间复杂环境有限时间内多机器人协作消杀作业动态调度与规划难题，从而为医院无人化消杀作业的装备部署与任务调度提供了有效的理论依据与技术支撑。

基于上述模型与算法，结合疫情期间武汉火神山医院和武汉大学人民医院两家医院的实际地图数据，开展了相关仿真实验研究。采用 MATLAB 开展了 A*算法与 RRT 算法的全局路径规划的对比仿真实验，实验结果表明，A*算法比 RRT 算法规划的轨迹更加平滑。采用 MATLAB 完成了仅基于 A*算法的动态避障仿真实验，由实验结果可知，仅使用 A*算法可实现动态避障，但需多次规划全局路径，导致计算量增大。通过 Webots 与 Python 联合的方式，验证 A*融合 DWA 的动态避障算法，实验结果表明，A*-DWA 算法可以很好的实现动态环境路径规划与避障。

据此，通过仿真实验手段，在三种不同约束条件下完成了机器人的优化调度，并基于 2 个医院隔离区地图实际数据开展了消杀机器人全局路径规划、动态实时路径规划和跟踪仿真验证，验证了所提控制方法的可行性和有效性。

7 参考文献

[1] 实时更新：新型冠状病毒肺炎疫情地图 [OL]. https://voice.baidu.com/act/newpneumonia/newpneumonia/?from=osari_aladin_banner#tab4. 2021 年08 月 19 日.

[2] 姜峰, 闫强明. 北大经院学者“新冠疫情对经济影响”笔谈综述 [J]. 经济科学, 2020, (2): 130-136.

[3] 黄中翔, 马林, 刘天昀, 张慧媛. 新冠肺炎疫情对世界经济政治的影响 [J]. 产业创新研究,2020 (7): 34-36.

[4] 邱东晓, 张黎聪. 从医护人员受感染看医疗机器人的发展 [J]. 医院与医学, 2020 (1): 1-4.

[5] 人权组织：墨西哥医护人员新冠死亡人数全球第一，美国第二|美国|印度|巴西_新浪科技_新浪网 [OL]. https://tech.sina.com.cn/roll/2020-09-04/doc-iivhuipp2489030.shtml. 2020 年 09 月 04 日.

[6] 徐宝丽, 管甲亮, 术超, 于涛, 骆锋, 曹学雷, 王永彬, 周长勇. 新型冠状病毒 COVID-19 相关研究进展 [J]. 中华医院感染学杂志, 2020, 30 (6): 839-844.

[7] 丁志虎, 胡光阔. 智能机器人在医院消毒作业中的应用 [J]. 医学信息学, 2020, 33 (5): 28-29.

[8] 董朝瑞, 郭欣, 李宁, 邵谢宁. 基于改进 A* 算法的多机器人动态路径规划 [J]. 高技术通讯, 2020, 30 (1): 71-81.

[9] 王甜甜. 多移动机器人路径规划及仿真研究[D]. 博士学位论文, 西安: 西安理工大学, 2019.

[10] 姚冲, 高兴莲, 吴荷玉, 杨英, 黄靖. 智能化消毒机器人在新型冠状病毒肺炎患者术后手术间消毒效果的评价 [J]. 中国医学装备, 2020, 17 (6): 174-176.

[11] 中国测评机器人国评中心. 奋战在抗疫前线的“钢铁战士” [J]. 机器人产业, 2020 (2): 90-109.

[12] 王一凡. 医护机器人在重大疫情中的应用探索 [J]. 企业技术实践, 2020 (4): 62-64.

[13] 成静, 杨旭, 陈洁雅. 智能消毒机器人在新型冠状病毒性肺炎隔离病房护理使用体验的研究 [J]. 科技与创新, 2020, 13: 28-31.

[14] Shatalov M, Lunev A, Hu X, Sun W, Jain R, Yang J, Dobrinsky A, Deng J, Bilenko Yu, Moe C G, Wraback M, Shur M and Gaska R. Efficient UV emitters for sensing and disinfection [C]. In: Proceedings of Conference on Lasers and Electro Optics, San Jose, California, United States OSA, 2012: JTh1L.4

[15] Mathebula T, Leuschner F W, Chowdhury S P. The use of UVC-LEDs for the disinfection of mycobacterium tuberculosis [J]. In: Proceedings of IEEE PES/IAS Power Africa, 2018, 739-744.

[16] Yang G Z, Nelson B J, Murphy R R, et al. Combating COVID-19—the role of robotics in managing public health and infectious diseases. Science Robot, 2020, 5: eabb5589.

[17] Chanprakon P, Saeoung T, Treebupachatsakul T, Hannanta-anan P, Piyawattanametha W. An ultra-violet sterilization robot for disinfection [C]. In: Proceedings of the 5th International

Conference on Engineering, Applied Sciences and Technology (ICEAST), 2019.

[18] 刘京运. 疫情当前, 钛米机器人增援一线 [J]. 机器人产业, 2020, 2: 60-63.

[19] 张辉, 王耀南, 易俊飞, 钟杭, 刘理, 缪志强, 江一鸣. 面向重大疫情应急防控的智能机器人系统研究 [J]. 中国科学: 信息科学, 2020, 50 (7): 1069-1090.

[20] 新浪网. 杭电教授研发杀菌机器人驰援武汉大幅提升 CT 检测室消杀速度 [J]. 评价与管理, 2020, 18 (1): 59.

[21] 高飞. 不确定因素下配送路径优化问题研究 [D]. 博士学位论文, 北京: 北京交通大学, 2019.

[22] 蔡光跃, 董恩清. 遗传算法和蚁群算法在求解 TSP 问题上的对比分析 [J]. 计算机工程与应用, 2007, 43 (10): 96-98.

[23] 陈晓艳, 张东洋, 苏学斌, 代钰贺, 赵春东. 基于改进遗传算法和多目标决策的货拉优化策略 [J]. 天津科技大学学报, 2020, 35 (4): 317-333.

[24] 郑义彬,邱兴宇,孙源泽,刘立博. 基于遗传算法的冷链物流配送路径优化研究 [J]. 公路与汽运, 2020, 3: 49-52.

[25] 李军, 谢秉磊, 郭耀煌. 非满载车辆调度问题的遗传算法 [J]. 系统工程理论方法应用, 2000, 9 (3): 235-239.

[26] 曹思萌. 动态环境下移动机器人的路径规划算法研究 [D]. 哈尔滨工业大学, 2019.

[27] 孙汉昌, 朱华勇. 基于概率地图方法的无人机路径规划研究 [J]. 系统仿真学报, 2006, 18 (11): 3050-3054.

[28] Leng Z, Dong M Z, Dong G Q, et al. A rapid path planner for autonomous ground vehicle using section collision detection [J]. Journal of Shanghai JiaotongUniversity (Science), 2009, 14 (3): 306-309.

[29] 王殿君. 基于改进 A*算法的室内移动机器人路径规划 [J]. 清华大学学报(自然 5 版), 2012 (8): 1085-1089.

[30] 徐小强, 王明勇, 冒燕. 基于改进人工势场法的移动机器人路径规划 [J/OL]. 计算机应用: 1-5[2020-09-02]. http://kns.cnki.net/kcms/detail/51.1307.TP.20200731.0944.002.html.

[31] 任工昌, 胡小龙, 刘朋. 基于路径跟踪的拖车式移动机器人动态窗口法 [J/OL]. 计算机应用研究: 1-5 [2020-09-02]. https://doi.org/10.19734/j.issn.1001-3695.2019.09.0577.

[32] 郭娜, 李彩虹, 王迪, 张宁, 宋莉. 基于模糊控制的移动机器人局部路径规划 [J]. 山东理工大学学报(自然科学版), 2020, 34 (04): 24-29.

[33] 王韬. 基于小波神经网络模糊滑模控制的轮式移动机器人避障研究 [J]. 中国工程机械学报, 2020, 18 (03): 278-282.

8 致谢

本课题的选题来源于如何高效实施新冠疫情隔离病区消毒工作。疫情期间，我们了解到医务人员除了要完成繁重的临床医护工作以外，，还要担负医疗环境的消杀工作，这大大加重了医务人员的工作负担。着眼于这一现状，通过和指导老师交流和讨论确立了本课题的研究内容：隔离病区的消杀机器人优化调度与路径规划。

感谢山东省实验中学石磊老师在课题的选题、仿真实验等方面的指导。特别感谢山东大学控制科学与工程博士生导师宋锐教授在系统建模、论文结构、仿真实验以及论文撰写给予的指导。感谢山东大学齐鲁医院的医护人员给予临床消毒规范的专业指导。本课题是在指导老师悉心指导下完成，受疫情影响，我们在课题的研究过程中多次通过视频会议的形式进行交流，开拓了我们的思路，对课题的研究起到了推动作用也给予了我们的完成课题的信心。

在本次课题完成之际，感谢给予关心支持和无微不至照顾的家人，感谢所有给予帮助和鼓励的同学与朋友。

9 附件

Optimal scheduling and path planning of multiple robots for disinfection in isolation areas

Zhili Liu, Tianyou Xie

1. Shandong Experimental High School, Jinan, 250061, P. R. China

Abstract: In this paper, by investigating and analyzing the actual demand of disinfection tasks in isolation areas during the epidemic, a strategy of optimal scheduling and path planning for multiple disinfection robots in isolation areas is proposed. Based on Vehicle Routing Problem (VRP), the optimal scheduling model of multiple disinfection robots is established through comprehensive consideration of the power consumption of disinfection robots, tasks levels and starting positions. Based on this, genetic algorithm (GA) is used to determine the minimum number of robots required, the assignment of disinfection tasks and the sequence of disinfection. Then, global path planning and real-time dynamic obstacle avoidance are realized by A*-dynamic window algorithm (A*-DWA) for disinfection robots in isolation areas. This provides an effective optimal scheduling strategy and dynamic path planning algorithm for the disinfection of multiple robots in large and complex dynamic environment.

Finally, taking the actual maps of the isolation areas in several hospitals as research objects, numerical simulations and the simulation experiments in three-dimensional physical environment are carried out by MATLAB and Webots, respectively. The simulation results verify the effectiveness and applicability of the proposed strategy.

Key Words: Multiple disinfection robots, isolation areas, optimal scheduling, path planing, real-time dynamic obstacle avoidance

1 Research background and practical requirements

Corona Virus Disease 2019 (COVID-19) has rapidly swept across the globe since its emergence in December 2019. By August 19, 2021, the COVID-19 has caused more than 210 million infections and over 4.4 million deaths, and has become a global epidemic threatening hu-man security[1]. According to the authoritative assessment, the damage of COVID-19 will be far more harmful than the economic crisis or terrorism[2, 3]. Although huge resources have been put into the prevention and control of the epidemic, the explosively increasing infections lead to a growing shortage on healthcare, especially medical staff. Even worse, medical staff on the front lines are not only overworked, but also at great risk of being infected at any time[4]. According to the WHO report, medical staff account for about 10% of the total infections (about 1.4 million cases) all around the world, and seriously, until September 2, 2020, there are over 7 thousand medical staff died from COVID-19[5]. COVID-19 owns the characteristics of rapid spread, high infectivity and wide transmission, for which there is no confirmed effective treatment currently[6]. Whereas, what's clear, the Corona Virus mainly spreads through the air, and the disinfection of risk areas (especially isolation areas) can prevent its spread effectively. Therefore, disinfection is one of the most important works to prevent and control COVID-19 in isolation areas. In practice, the main disinfection methods include ultraviolet irradiation and hydrogen peroxide/sodium hypochlorite disinfectant spraying[7], and moreover, the traditional disinfection is mainly accomplished by manual operation. It is necessary to point out that ultraviolet irradiation disinfection requires the evacuation of people on the scene and makes many sterile blind areas are left due to the limited exposure range. In addition, the highly corrosive and high-concentration hydrogen peroxide/sodium hypochlorite disinfectants threatens the disinfection workers' safety. Meanwhile, the high frequency spraying in isolation areas brings heavy workload to the disinfection workers.

With the development of intelligent robot technology, robot systems in complex environment have played an increasingly important role in military, industry, agriculture, medicine, to name a few[8–11] . Particularly, in the medical field, a variety of medical service robots, such as the targeted therapy micro-robot[9], the disinfection robot[10], the guiding robot and the indoor delivery robot[11], have played a crucial role in the disease diagnosis, as well as the epidemic prevention and control. According to a study of the Artificial Intelligence Industry Alliance, intelligent service robots, as the most commonly used intelligent products in the prevention and control of COVID-19, have been used to solve many problems exposed in the fight against COVID-19, such as the lack of medical staff and the untimely delivery of medical supplies. Particularly, as a representative kind of intelligent service products, the disinfection robots have been widely used in the isolation areas[12]. With the high mobility, low energy consumption and high fault tolerance, disinfection robots can not only alleviate the heavy workload but also reduce the infection rates of medical staff in the disinfection process[13]. At the same time, compared with manual operation, the robot can effectively improve the efficiency of disinfection work. Therefore, it is of great significance for the prevention and control of COVID-19 to deeply investigate the disinfection robots and their optimal operation.

In recent years, the intelligent disinfection equipment have been gradually used in practice[14–17]. Specifically, in 2012, Shatalov et al.[14] designed a ultraviolet emitter with effective disinfection ability. The feasibility of portable ultraviolet devices and intelligent disinfection robots was verified in [15, 16]. In 2015, an ultraviolet disinfection robot produced by Chenix disinfection services (U.S.) has already been applied to the front line of the fight against Ebola,

which can protect the medical staff from infection. Moreover, Chanprakon developed an ultraviolet disinfection robot with autonomous obstacle avoidance ability to accomplish the 360° disinfection of operating rooms or wards[17].

In our country, intelligent disinfection robots have been applied in the fight against COVID-19. For example, by integrating hydrogen peroxide spraying, ultraviolet irradiation and plasma air filtration, the disinfection robot developed by Shanghai Timi Robot Technology accomplished the disinfection work in multiple scenes[18]. The disinfection robot produced by Shanghai Fantong Biological Technology has been successfully applied to the wards and operating rooms, by combining the hydrogen peroxide disinfection and artificial intelligence technology. The robot developed by the State Key Laboratory of Hunan University and Hunan Aimijia Intelligent Technology Company can realize the ward disinfection through ultraviolet light and disinfectant spraying, as well as owning autonomous navigation[19]. The ultraviolet disinfection robot developed by Hangzhou University of Electronic Science and Technology can achieve efficient ultraviolet sterilization and automatic path planning[20]. The disinfection robot developed by DaLuZhiYuan Technology with sodium hypochlorite as the disinfectant can automatically adjust such parameters as disinfection concentration and spray form according to the environmental information, which has been applied to the front line of anti-epidemic in Huanggang Maternal and Child Health Hospital, Central Hospital of Huanggang and Wuhan Union Hospital.

Although disinfection robots have achieved some field applications during the epidemic, according to the survey just completed, most of the existing robots cannot effectively solve the disinfection task of the isolation wards, and there are common problems such as low intelligence level and poor adaptability. The robot operation mode is mainly single machine operation and fixed path. It is difficult to deal with multiple machine cooperative tasks in large complex scene, especially lack of effective solutions for the daily multiple frequency disinfection tasks with time constraint required in the actual disinfection operation, and the real-time processing of dynamic obstacles in the working environment.

Under the urgent situation of the rapid spread of the new crown virus, aiming at the practical problems such as single disinfection mode, high energy consumption and long disinfection time of COVID-19 anti-epidemic robots, after considering the remaining power of the disinfection robots, disinfection tasks in key areas and initial positions comprehensively, this paper proposes an optimal scheduling strategy for multiple disinfection robots in isolation wards with multiple constraints based on the VRP model. In view of the particularity of the isolated ward environment, a multiple robot path planning control algorithm combining A*-DWA is proposed to realize global path planning in known environment and local real-time dynamic obstacle avoidance in unknown environment. According to the actual data of the isolation ward map of Wuhan Huoshenshan Hospital and RHWU, a 3D simulation environment was built. The global path planning, dynamic real-time path planning and tracking experiments of multiple disinfection robots are carried out respectively to verify the feasibility and effectiveness of the proposed control method.

2 Description of disinfection task for multiple robots

This paper aims at investigating the optimal scheduling and path planning of multiple disinfection robots in isolation areas under the architecture shown in Figure 1. Each disinfection robot starts from the charging station, and returns after completing the assigned disinfection task. Besides, according to the disinfection standards of hospitals, each single disinfection task should be completed within prescribed time. Then, under the constraints of each robot on the load, the remaining power and the disinfection task in key areas, the optimal scheduling strategy is proposed to render the number of required robots minimum and the moving paths shortest in the task, and to determine the sequence of disinfection wards for each robot.

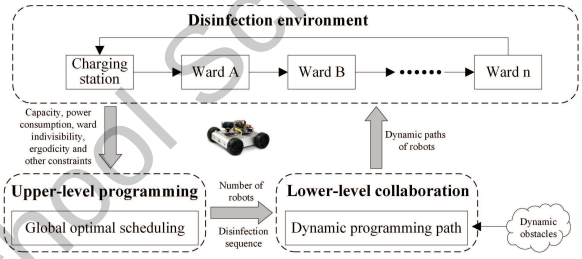

Figure 1. Optimal scheduling and path planning of disinfection robots.

In what follows, the location and required disinfectant amount of each ward, the walking speed and power consumption per unit distance of the robots, and the locations of charging stations are all supposed known. In addition, suppose that in one disinfection period, each ward is disinfected by one robot only once. Then, the multi-robot disinfection task can be taken as a typical problem of optimal scheduling with multiple constraints and path planning in complex environment. According to the disinfection requirements in isolation areas, the optimal scheduling strategy of multiple disinfection robots is proposed under the constraints on energy consumption, ward environment and disinfection task. Based on this, a novel strategy of path planning is presented by A*-DWA to achieve the global optimal dynamic obstacle avoidance for multiple robots in disinfection process.

3 Optimal scheduling of multiple disinfection robots

This section is devoted to the modeling and analysis of the optimal scheduling of multiple disinfection robots. Specifically, the model of the optimal scheduling of multiple disinfection robots with multiple constraints is first established by using VPR model. Based on this, the optimal scheduling problem is solved by using GA flexibly.

3.1 Modeling of optimal scheduling of multiple disinfection robots

The optimal scheduling problem of disinfection robots with multiple constraints in isolation areas is modeled by

VRP[21]. The main objective of the optimal scheduling is to determine the minimum number of robots required and the optimal scheduling in the isolation areas, that is, to render the assigned disinfection task completed within the specified time by using as few robots as possible while the total path is the shortest.

Based on the graph theory, define an undirected graph $G = (V, E)$, where $V = \{0, 1, \ldots, n\}$ denotes the set of all the nodes in isolation areas, with 0 being the charging station node and $\{1, \ldots, n\} =: V'$ being the set of all the isolation ward nodes; E is the set of edges, that is, $E = \{(i, j)|i, j \in V, i \neq j\}$ with the weight of each edge c_{ij} $(i, j \in V, i \neq j)$ denoting the shortest path from node i to node j. Moreover, the following assumptions are made:

Requirement:

The amount of disinfectant d_i required for isolation ward i is fixed, and there is enough disinfectant at the nurse station.

Multiple robots:

The set of robots required for disinfection task is denoted by $K = \{1, \ldots, m\}$, where all the robots are of the same type and have the same disinfectant capacity Q. Besides, the remaining power of robot k is denoted by P_k, $k = 1, \ldots, m$.

Constraint conditions:

① Each robot starts from the charging station and returns after completing all the assigned disinfection task.

② The whole disinfection task of each isolation ward is completed by only one robot in a disinfection period.

③ The total amount of disinfectant needed in the task chain doesn't exceed the robot capacity, and each disinfection task chain has at least one isolation ward node.

④ The total power consumption for the disinfection work on the task chain is less than or equal to the remaining power of the robot.

⑤ The disinfection work on each task chain is completed within the specified time.

The parameters and variables involved in the optimal scheduling problem are defined in the following Tables 1 and 2.

Table 1. Interpretations of sets

Sets	Interpretations
$V = \{0, 1, \ldots, n\}$	The set of all the nodes in isolation areas, (0 denotes the charging station node)
$V' = \{1, \ldots, n\}$	The set of all the isolation ward nodes
$K = \{1, \ldots, m\}$	The set of the disinfection robot
S_k	The set of all the isolation ward nodes that on the assigned task chain of robot k

Decision variables:

$$x_{ijk} = \begin{cases} 1, \text{ if robot } k \text{ moves from node } i \text{ to node } j, \\ 0, \text{ else.} \end{cases} \quad (1)$$

Objective function:

Table 2. Interpretations of parameters

Parameters	Interpretations
c_{ij}	The weight of edges, i.e., the shortest path from node i to j, $(i, j \in V, i \neq j)$
Q	The disinfectant capacity of each robot (maximum load capacity)
d_i	The amount of disinfectant required for isolation ward i
P_k	The remaining power of robot k
λ_1	The amount of power that a robot consumes for moving a unit distance
λ_2	The amount of power that a robot consumes for disinfecting an isolation ward
t_1	The time that a robot spends on moving a unit distance
t_2	The time that a robot spends on disinfecting an isolation ward
T	The time specified for robots to complete disinfection task in isolation areas

$$\min F = \sum_{k \in K} \sum_{i \in V} \sum_{j \in V} c_{ij} x_{ijk} \quad (2)$$

s.t.

$$\sum_{i \in V} x_{0ik} = 1, k \in K, \quad (3)$$

$$\sum_{i \in V} x_{ilk} = \sum_{j \in V} x_{ljk}, l \in V, k \in K, \quad (4)$$

$$\sum_{j \in V} x_{j0k} = 1, k \in K, \quad (5)$$

$$\sum_{k \in K} \sum_{i \in V} x_{ijk} = 1, j \in V', \quad (6)$$

$$\sum_{k \in K} \sum_{j \in V} x_{ijk} = 1, i \in V', \quad (7)$$

$$\sum_{i \in S_k} \sum_{j \in S_k} x_{ijk} d_i \leq Q, k \in K, \quad (8)$$

$$\sum_{i \in S_k} \sum_{j \in S_k} \lambda_1 c_{ij} x_{ijk} + \lambda_2 |S_k| \leq P_k, k \in K, \quad (9)$$

$$\sum_{i \in S_k} \sum_{j \in S_k} x_{ijk} \leq |S_k| - 1, k \in K, \quad (10)$$

$$\sum_{i \in S_k} \sum_{j \in S_k} t_1 c_{ij} x_{ijk} + t_2 |S_k| \leq T, k \in K, \quad (11)$$

$$x_{ijk} \in \{0, 1\}, i, j \in V, k \in K. \quad (12)$$

Equations (3)-(5) indicate that each robot starts from the charging station and transfers to the next ward after disinfecting one isolation ward node on the task chain, and returns to the charging station after completing all the disinfection works on the task chain. Equations (6) and (7) mean that each isolation ward is disinfected only once by one robot during a disinfection period. Equation (8) means that the total amount of disinfectant for isolation wards on each task chain doesn't exceed the maximum capacity of the robot. Equation (9) indicates that the power amount that the robot consumes for the disinfection work on the task chain is less than or equal to its remaining power amount. Equation (10)

is a branch elimination constraint. Equation (11) indicates that the total time required by the robot to complete the disinfection work on the task chain cannot exceed the specified time. Equation (12) represents the attribute of decision variables.

3.2 Optimal scheduling strategy of multiple disinfection robots

The common algorithms of optimal scheduling include Ant Colony Optimization (ACO)[22], Generic Algorithm (GA) [23], etc. ACO is a greedy heuristic algorithm with the disadvantage of slow convergence speed and the solution obtained by it is usually local optimal, rather than global optimal. GA can effectively achieve the global search in the sense of probability, with the advantages of inherent parallelism and global optimization. Moreover, GA can also optimize search space and adjust the search direction adaptively. For the system model proposed in Section 3.1, GA is adopted to solve the optimal scheduling problem under investigation. The calculating steps are as follows:

Coding scheme design:

Note that VRP is a discrete optimization problem. Then, combining constraint conditions (6) and (7), we code the wards by natural numbers[24, 25]: Let 0 denote the charging station node, $1, \ldots, n$ denote the isolation ward nodes, and if the number of disinfection robots required is k; correspondingly, the chromosome length is $n + k + 1$.

Population initialization:

We first randomly line up all the ward codes, and let q_i represent the power consumption of the ith ward node in chromosome. If $\sum_{i=1}^{a} q_i \leq Q$ and $\sum_{i=1}^{a+1} q_i > Q$, then 0 is inserted behind the ath position of chromosome, and after inserting 0, repeat the calculation until the last code. Subsequently, we insert 0 at both the first and the last positions of chromosome to generate an initial chromosome. Repeating the above steps N times, the desired initial population with N individuals are constructed, where N is the number of individuals in initial population .

Constraint handling and fitness function:

Under constraint conditions (3)-(5) and (8)-(9), we decode the chromosome into the disinfection paths of robots. Based on the disinfection paths, once the first robot reaches the first ward and completes the disinfection task, it should be determined that whether the remaining power of the robot can make sure that the robot can return to the charging station. If this condition is still satisfied after adding ward 2 into the path of the first robot, the path of the first robot will be $0-1-2-0$. By analogy, once the conditions are violated, one new robot is added to the task, that is, the second route from the charging station will be designed.

According to the decoded disinfections path of robots, the objective function given in (2) is calculated. Since the fitness function is the larger, the better, we take the reciprocal of the objective function (2) as fitness function. That is,

$$fit(i) = \frac{1}{\sum\limits_{k\in K}\sum\limits_{i\in V}\sum\limits_{j\in V} c_{ij}x_{ijk}}. \tag{13}$$

Moreover, it is necessary to determine whether the power consumption (for disinfection and walking) of the robot exceeds the total power. If the power consumption exceeds the total power, then the disinfection path is infeasible, and the corresponding solution is called an infeasible one, which can be eliminated by increasing the target value via the penalty function.

Genetic operation:

(i) *Selection and copy*

By using the roulette selection method, we replace the worst chromosome of offspring by the best one of the paternal. Then, calculating the sum of fitness functions of all chromosomes in the current population, it gives

$$sum\ fit(i) = \sum_{i}^{n} fit(i). \tag{14}$$

Calculating the selection probability of each chromosome in the current population, we have

$$p(i) = \frac{fit(i)}{sum\ fit(i)},\ i \in N. \tag{15}$$

Furthermore, calculating the cumulative probability of each chromosome in the current population, it follows that

$$ps(i) = \sum_{i\in N} p(i). \tag{16}$$

For a real number r randomly generated in interval $[0, 1]$, if $ps(i) > r$, we choose the first chromosome, and otherwise, choose the ith chromosome, where i satisfies $ps(i-1) < r < ps(i)$.

(ii) *Chromosomes crossover*

Two sub-routes A and B are first randomly selected on paternal chromosomes 1 and 2, respectively. Then, the selected sub-routes are put forward, and the sub-route A of the paternal chromosome 1 is taken as a part of the offspring chromosome 1. Meanwhile, the code that does not appear in the sub-route A of the paternal chromosome 2 is added behind the sub-route A according to the order of the paternal chromosome 2, and the code 0 is added at the end of the chromosome. Finally, for the offspring chromosome 1, the part after sub-route A is randomly interrupted many times. The fitness of all cases is calculated respectively, and the largest fitness value is taken as the offspring chromosome 1. In the similar way, the offspring chromosome 2 can be obtained.

(iii) *Chromosome mutation*

The 3-exchange mutation operator is used to mutate the chromosome. Specifically, three randomly selected positions in the paternal chromosome are exchanged, and five offspring chromosomes are then obtained. By calculating the fitness for all cases, the offspring chromosome with highest

fitness enter the offspring population.

Terminating conditions:

Since GA is a random search algorithm, certain terminating rule must be pre-set to terminate the evolutionary cycle of the algorithm. There are three common terminating rules: (i) A prescribed goal is achieved; (ii) The optimal individual in the population is no longer improved in successive generations, (iii) The preset number of evolutions has been reached. To guarantee the accuracy of solutions and the running time of the algorithm effectively, the pre-determined evolutionary times is chosen as the termination rule in this paper.

4 Path planning of multiple disinfection robots in isolation areas

Path planning is the premise of the efficient and autonomous robot operation, which aims at making the robot move along the optimal path in a complex environment. According to the information acquired from the environment, path planning can be divided into static global path planning and local path planning of dynamic obstacle avoidance. Global path planning is, based on the established global map, to provide a static optimal path from the starting point to the end point. Local path planning of dynamic obstacle avoidance is, based on the detection of local surrounding environment through sensor, to enhance the real-time adaptability and the capacity of obstacle avoidance. Therefore, it is of great theoretical and practical significance to integrate the strategies of static global path planning and local path planning of dynamic obstacle avoidance.

4.1 Static global path planning algorithm for multiple robots

In the implementation of practical task, static global path planning is required for ensuring the shortest path for disinfection robots from the initial position to the target one. The common algorithms on static global path planning include ones based on sampling and ones based on graph search, where the former include probabilistic road map algorithm (PRM) and rapidly-exploring random tree algorithm (RRT algorithm), and the latter include Dijkstra algorithm (D algorithm) and A* algorithm. The precision of PRM algorithm depends on the number of randomly selected nodes: when the number of nodes is large, the optimal solution can be obtained, but the calculation amount would be increased and the efficiency would be reduced[26]. RRT algorithm, applicable to the path planning in the multi-dimensional space, determines a path by randomly sampling the road points in the space, through which, however, the path obtained is seldom optimal[27]. D algorithm can find the shortest path from the starting point to the outer layer and then to the end point, but with a blind search strategy adopted, makes many meaningless points involved in the search process so as to result in the high time complexity and low computational efficiency[28]. A* algorithm, as a classical heuristic search algorithm, is to find the global shortest route in the static environment by expanding the node with the minimum heuristic function, and can ensure the global optimal solution sought[29]. Moreover, compared with D algorithm, the search efficiency of A* algorithm is significantly enhanced. This motivates us to seek the desirable path for disinfection robots by using A* algorithm.

A* algorithm principle:

The path search space is first divided into a grid, and the next path location is gradually determined by comparing the cost functions of eight adjacent points of the current location. As shown in Figure 2, the blue circle represents the current location node, numbers $1, \ldots, 8$ represent the eight adjacent nodes of the current location, and the blue arrows represent possible choices from the current location to the next one.

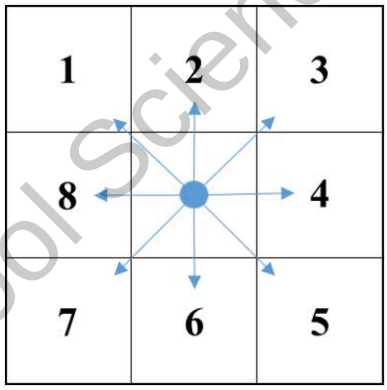

Figure 2. Search procedure of A* algorithm.

Algorithm flow:

The flow of A* algorithm is shown in Figure 3. Specifically,

(i) Initialize related parameters; generate the open list and close list; set the range of search space.

(ii) Based on the open list, check whether the target location is included. If so, finish the path planning, and otherwise, execute the next step.

(iii) Calculate the cost function of each point in the open list; find out the point corresponding to the minimum value; set the point as the current node; add the node to the close list. The expression of the cost function is in the following form:

$$F(n) = g(n) + h(n), \tag{17}$$

where n is the current point; $g(n)$ is the actual cost value from the initial location of the path to the current point; $h(n)$ is the estimated cost value (i.e., heuristic function) from the current point to the target location of the path.

(iv) Analyze and calculate the eight adjacent points around the current one.

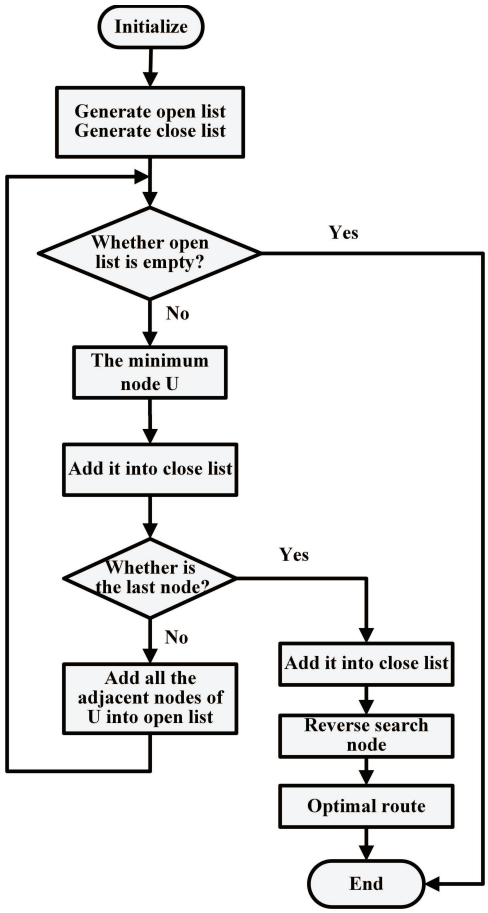

Figure 3. Flow block diagram of A* algorithm.

① If the point is an obstacle, or is in the close list, it will not be considered, and otherwise, turn to the next step.
② If the point is not in the open list, add it into the open list; set the current node as the paternal node; record the cost function of the point.
③ If the point is in the open list, check whether it is the optimal path to move to the point (the smaller the $g(n)$, the better the path). If so, keep the point and set the paternal node of the node as the current node; recalculate the cost function of the point.

(v) Return to step (ii).

In the above search process, the open list records all the points that the robot possible passes through, and the close list records the location points that the robot passes through.

4.2 Local dynamic obstacle avoidance algorithm for disinfection robots

In the isolation areas, there are inevitably dynamic obstacles such as medical staff and temporary stacking objects. Therefore, the disinfection robots in this area should be able to realize dynamic obstacle avoidance. The common dynamic obstacle avoidance algorithms include artificial potential field (APF)[30], DWA[31], fuzzy control[32] and neural network[33], to name a few. APF is frequently used in the path planning because of its simple algorithm, but the selection of gravitational field and repulsion field in the algorithm makes the robot fall into the local optimum, which will cause the breakdown of the robot. The idea of DWA is to search the optimal control command to maximize the objective function group. Particularly, by sampling multiple groups of speeds in the speed space and simulating the trajectories of the robots with these speeds in a certain period of time, multiple groups of trajectories can be obtained. Then, evaluating these trajectories yields the optimal one, and the robot is driven with the speed corresponding to the optimal trajectory to achieve dynamic obstacle avoidance. Remark that DWA can achieve the environmental detection in real-time and the selection of appropriate forward strategy based on its own sensors, which owns the advantages of low calculation amount and high real-time performance, and can be flexibly combined with other path planning algorithms.

In this paper, we employ DWA to realize local dynamic obstacle avoidance. In the 2-dimensional plane, the robot position can be translated into a function of linear velocity and angular velocity.

In the continuous case:

$$x(t_n) = x(t_0) + \int_{t_0}^{t_n} v(t)\cos\theta(t)\mathrm{d}t, \quad (18)$$

$$y(t_n) = y(t_0) + \int_{t_0}^{t_n} v(t)\sin\theta(t)\mathrm{d}t, \quad (19)$$

$$\theta(t_n) = \theta(t_0) + \int_{t_0}^{t_n} \omega(t)\mathrm{d}t, \quad (20)$$

where $v(t)$ is the linear velocity; $\theta(t)$ is the heading angle; $\omega(t)$ is the angular velocity.

In the discrete case:

$$\Delta x = v_x\Delta t\cos\theta_t - v_y\Delta t\sin\theta_t, \quad (21)$$

$$\Delta y = v_x\Delta t\sin\theta_t + v_y\Delta t\cos\theta_t, \quad (22)$$

$$\Delta\theta_t = \omega_t\Delta t, \quad (23)$$

where v_x and v_y are components of the linear velocity along the x-axis and y-axis, respectively; θ_t is the heading angle; ω_t is the angular velocity.

Constraint conditions:

① The maximum and minimum velocities constraints.

The linear velocity and angular velocity of robots satisfy the corresponding constraints. Based on this, define

$$V_m = \left\{(v,\omega)|v \in [v_{\min}, v_{\max}] \wedge \omega \in [\omega_{\min}, \omega_{\max}]\right\}, \quad (24)$$

where $v_{\min}$ and $v_{\max}$ are the minimum and maximum linear velocities of robots, respectively; $\omega_{\min}$ and $\omega_{\max}$ are the minimum and maximum angular velocities of robots, respectively.

② The acceleration and constraints.

During the robot forward period, the dynamic window V_d is defined as follows:

$$V_d = \left\{(v,\omega)|v \in [v_c - \dot{v}\Delta t, v_c + \dot{v}\Delta t] \wedge\omega \in [\omega_c - \dot{\omega}\Delta t, \omega_c + \dot{\omega}\Delta t]\right\}, \quad (25)$$

where v_c and ω_c are the linear velocity and the angular velocity of robots, respectively; $\dot{v}$ and $\dot{\omega}$ are the acceleration

and angular acceleration of robots, respectively; Δt is the action time of acceleration $\dot{v}$ and angular acceleration $\dot{\omega}$.

③ Braking distance constraints.

To ensure safety, the robot should reduce the current speed to zero with the maximum deceleration before hitting the obstacle. Define

$$V_a=\left\{(v,\omega)|v\leq(2dist(v,\omega)\dot{v}_b)^{\frac{1}{2}},\omega\leq(2dist(v,\omega)\dot{\omega}_b)^{\frac{1}{2}}\right\}, \tag{26}$$

where $dist(v,\omega)$ is the closest distance from the robot to the obstacle.

Evaluation function:

Since there are several groups of feasible sampling speeds in the velocity space, it is necessary to design an evaluation function to select the optimal trajectory. The design criteria of the evaluation function is to make the robot move towards the target as fast as possible with the premise of avoiding obstacles. Correspondingly, the evaluation function is given in the following form:

$$G(v,\omega)=\sigma\big(\alpha head(v,\omega)+\beta dist(v,\omega)+\gamma vel(v,\omega)\big), \tag{27}$$

where $\sigma(\cdot)$ is a smooth function; $head(v,\omega)$ is the evaluation function of azimuth, which represents the azimuth deviation between the end direction of trajectory and the target under the current velocity; $dist(v,\omega)$ denotes the nearest distance from the obstacle to the trajectory (corresponding to the velocity); $vel(v,\omega)$ is the evaluation function of the current velocity and α,β,γ are the weighted coefficients.

4.3 Dynamic path planning for multiple disinfection robots based on A*-DWA

Despite being the the most effective algorithm of static global path planning, A* algorithm cannot cope with the obstacles that may arise at any time. DWA is equipped with the ability of obstacle avoidance, but apt to fall into the fatal problem of local optimum, without taking the requirement on static global optimal path into account.

A* algorithm is one of the most effective search algorithms to plan the shortest path in static environment, but it is hard to deal with dynamic obstacle avoidance. DWA can achieve online real-time planning path based on local window environment information detected by mobile robots, hence it owns the ability of obstacle avoidance. However, DWA can not make sure the achievement of global optimal path planning, which makes the planned path local optimal, rather than global optimal. Therefore, this paper develops a novel dynamic path planning strategy combing A*-DWA to ensure the global optimization of dynamic planning path. The algorithm flow is shown in Figure 4.

We now transform $head(v,\omega)$ in (27) into $PHead(v,\omega)$, where $PHead(v,\omega)$ is the azimuth deviation between the current target position and the end position, and the current target point is the sequence point on the global optimal path closest to the current position.

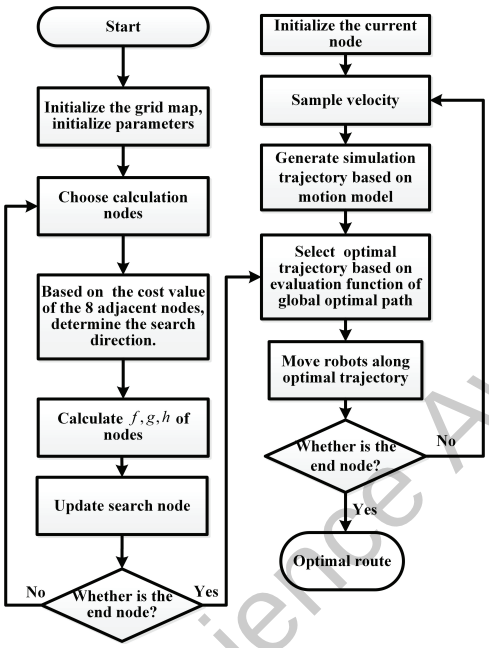

Figure 4. Search procedure of A*-DWA.

Accordingly, the evaluation function can be rewritten as

$$G(v,\omega)=\sigma\big(\alpha PHead(v,\omega)+\beta dist(v,\omega)+\gamma vel(v,\omega)\big), \tag{28}$$

which can not only ensure the local path planning to follow the global optimal path, but also render the robots to achieve dynamic obstacle avoidance along the global optimal path.

5 Simulation and verification of multiple disinfection robot system

According to the maps of the isolation areas of Huoshenshan Hospital and RHWU, the simplified simulation maps are designed correspondingly, as shown in Figure 5. The length and width of each ward in isolation area is $3m$ and $2m$. the width of ward corridor is $1.5m$, and the width of hall corridor is $6.4m$. The simulation experiment environment is designed based on the above data.

Combing with the disinfection tasks of four isolated areas, MATLAB and Webots+Python are used to verify the proposed algorithm. It should be pointed out that All the following simulation experiments are carried out on the 16GB RAM, Intel Core$^{\mathrm{TM}}$ i5-8265U CPU, Windows 10 64 bit operating system.

5.1 Simulations of optimal scheduling strategy of multiple disinfection robots in isolation areas

In this experiment, by considering the constraint conditions of remaining power, disinfection tasks in key areas and initial positions, GA is applied to solve the optimal scheduling strategy of multiple disinfection robots. In GA based on the natural number coding, we suppose that the initial population size is 100, the maximum iteration time is 200, the crossover probability P_c is 0.9, and the mutation probability P_m is 0.1. We also suppose that the Huoshenshan Hospital isolation area is assumed to be composed of four units: A,

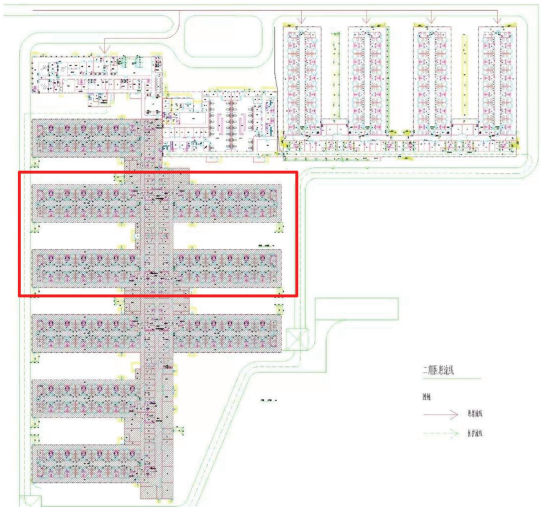

(a) Plane graph of Huoshenshan Hospital.

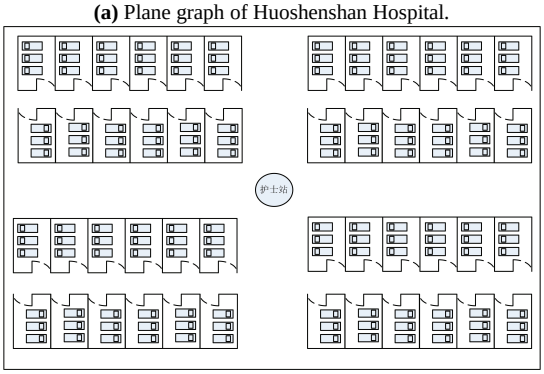

(b) Ketch of the isolation area.

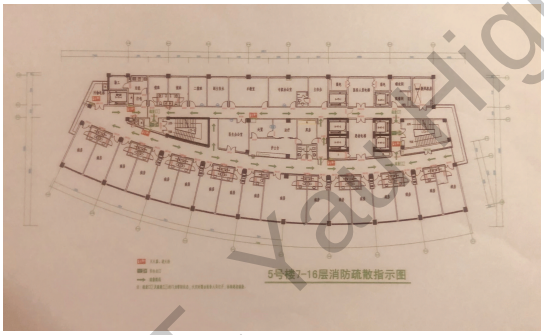

(c) Plane graph of RHWU.

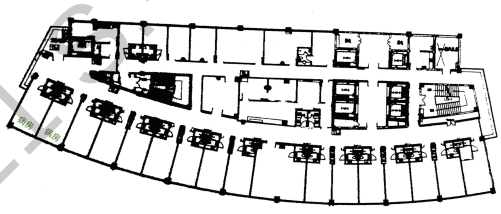

(d) Sketch of the isolation area.

Figure 5. Designed maps of isolation areas.

B, C and D, and each area has 12 wards with the same structure. In Figure 6, the black point in the center represents the starting point (and the ending point at the same time) of the robot (i.e., the charging station), and each other points represent the central positions of different wards. The closed graph with the same color represents the scheduling strategy of a robot, and the closed graph represents the optimal scheduling strategy of the robot planned by GA under the constraint conditions with the closed graphs, with different colors being the disinfection paths of different robots.

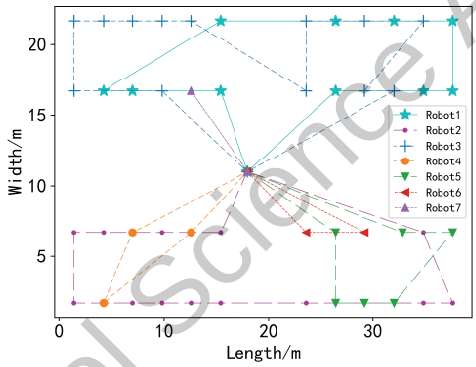

(a) Task allocation of robot with 20Ah remaining power.

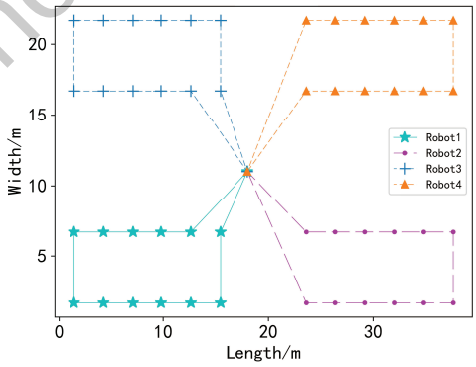

(b) Task allocation of robot with 40Ah remaining power.

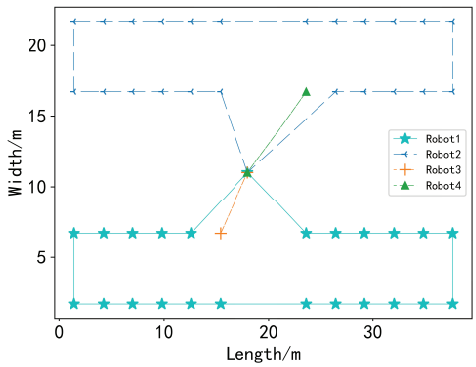

(c) Task allocation of robot with 60Ah remaining power.

Figure 6. Optimal scheduling with different remaining powers.

Experiment I:

We assume that each disinfection robot is equipped with a power lithium battery and the power consumption for the disinfection of each ward is fixed: 1Ah. It is sup-

posed that the robot walking path is linear with the power consumption, and the preset ratio is 1:1. In three cases that the remaining powers of the robots are both 20Ah, 40Ah and 60Ah, by using GA, the minimum number of the assigned disinfection robots and the corresponding disinfection sequences are determined. The results of the optimal scheduling under the same disinfection task but under the different initial remaining powers of the robots are shown in Figure 6, which indicates that the optimal numbers of robots in the three cases are7, 4 and 4 respectively.

The iteration processes of the optimal scheduling are shown in Figure 7, where the blue and red lines represent the values of the minimum and average objective functions in each generation, respectively. It is easy to see that the increase of iteration times, the objective function array decreases obviously and converges ultimately.

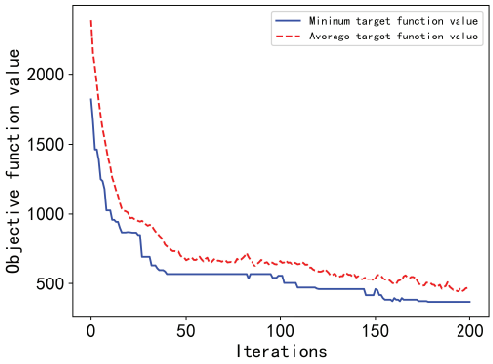

Figure 7. Optimal scheduling iterative process of GA.

Experiment II: When the remaining power of the robot is 40Ah, it is assumed that the 9 wards of isolation unit A and the 6 wards of isolation unit C need to be disinfected emphatically, that is, the power consumption of each ward in units A and C is doubled. The optimal scheduling result of the robots with the same initial power but different disinfection tasks is shown in Figure 8. It can be seen that, compared with Figure 6 (b), the optimal scheduling strategy is redesigned.

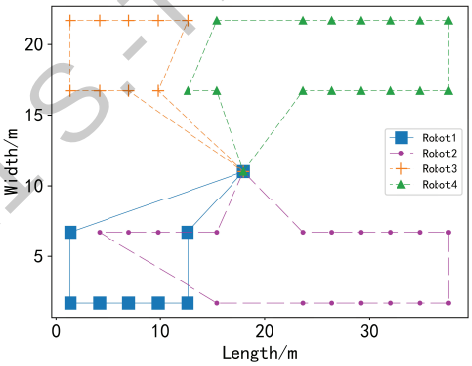

Figure 8. Task allocation of key disinfection wards.

Experiment III: Noting that the actual situations of different isolation areas are different, the initial positions of robots are usually different. Therefore, we consider the case that the initial positions of the robots (i.e., the positions of charging stations) changes. Suppose that the two charging stations are set between units A and B and between units C and D, respectively, and then,when the remaining power of the robots is 20Ah, the optimal scheduling is redesigned, as shown in Figure 9. It can be seen that the principle of proximity is adopted to ensure the optimal fitness function.

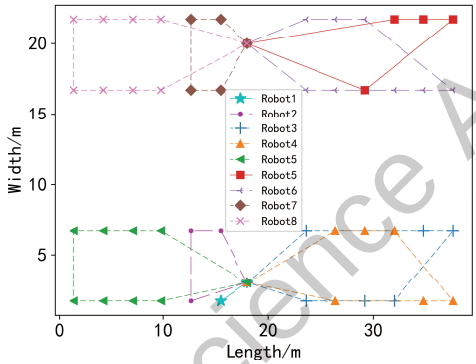

Figure 9. Optimal scheduling when charging stations are located in different positions.

5.2 Simulations of path planning and dynamic obstacle avoidance strategy of disinfection robots

Experiment I: In this experiment, under the condition that the global map is known, A* algorithm is used for the path planning of a single disinfection robot in the maps of isolation areas of Huoshenshan Hospital and RHWU (shown in (b) and (d) of Figure 5). To show the advantages of A* algorithm, a comparative experiment is carried out in Figure 5 (b) by using RRT algorithm. It is assumed that size of the robot is 0.4*0.4m^2; the running speed of the robot is 1 m/s; the turning radius is $1.5m$ and the sampling time T is $0.1s$. Let the initial state of the robot in the map shown in Figure 5 (b) is: Xstart = [19, 11, 0], Ygoal = [31, 16, 0] and the global search scope is $38 \times 22m^2$. Let the initial state of the robot on the map shown in Figure 5 (d) is: Xstart = [270, 120, 0], Ygoal = [90, 110, 0] and the global search scope is $500 \times 200m^2$. The global optimal paths planned are shown in Figure 10, where the green points are the starting positions of the robot and the red point represents the preset objective position of the robot. Particularly, Figure 10 (a) shows that the global path planned by A* algorithm is smooth and collision free. As shown in Figure 10 (b), RRT algorithm first traverses all the global random path points, and then determine the optimal path, which makes the amount of calculation is large, and the path path is not optimal and not smooth.

Experiment II: The optimal path planning of two disinfection robots A and B are achieved by using A* algorithm on the map shown in Figure 5 (b). It is assumed that size of the robot is 0.4*0.4m^2; the running speed of the robot is 1 m/s; the turning radius is $1.5m$, the sampling time T is $0.1s$ and the global search scope is $38 \times 22m^2$. By setting the starting positions of the robots A and B: Xstart1 = [19, 11, 0] and Xstart2 = [19, 10, 0], respectively, and the target positions: Ygoal1= [31, 16, 0] and Ygoal2 = [13, 2, 0],

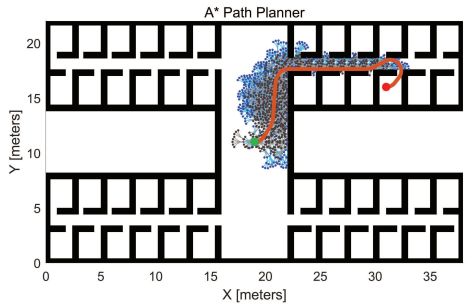

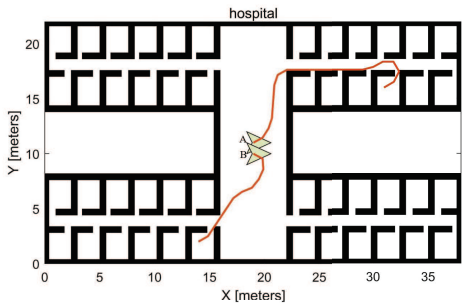

Figure 11. Obstacle avoidance paths of two disinfection robots planned A* algorithm.

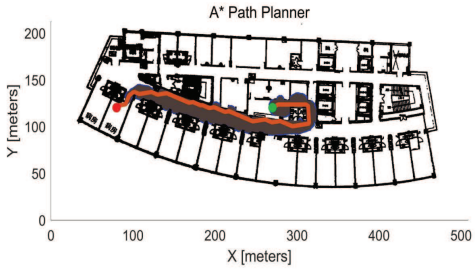

(a) Optimal path planned by A* algorithm.

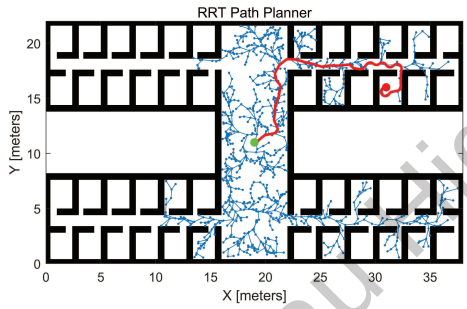

(b) Optimal path planned by RRT algorithm.

Figure 10. Optimal path of one robot.

respectively, the planned optimal paths are shown in Figure 11. It can be seen from the figure that A* algorithm realizes the global collision-free optimal path planning for two robots with different starting and end positions.

Experiment III: Suppose that the obstacles appear on the map after the robot has been running for 1 second, with the same parameters as in Experiment II of Subsection 5.2, the optimal path planning of robots A and B are obtained as shown in Figure 12 (a). Particularly, the blue and yellow areas are the vision fields that can be reached by the distance sensors of disinfection robots A and B, respectively (the darker the color, the closer the visual range). It can be seen from the figure that when two disinfection robots encounter one obstacle respectively, robot A performs path planning three times, while robot B performs path planning four times.

Suppose that a new obstacle appears on the walking path of robot a after its first-time obstacle avoidance, and then the disinfection robot will plan the optimal path once again, as shown in Figure 12 (b). At this time, robot A has completed five times of optimal path planning from the initial position to the target position.

From the above simulation experiments, it can seen that A* algorithm can effectively realize the global path planning based on the known map. However, when dynamic obstacles appear, the robot needs to replan the global path to avoid collision. This indicates that the real-time performance of A* algorithm is poor.

5.3 Simulations of global dynamic path planning based on A*-DWA in isolation areas

The simulation of physical components such as sensors in MATLAB is somewhat cumbersome. Therefore, the following experiments are carried out in the 3D physical simulation platform Webots + python. Webots is an open source physical simulation environment with physical simulation components close to the actual situation and rich sensor types.

In this experiment, 3D simulation experiments were carried out under the simplified map of the isolation areas of Huoshenshan Hospital and RHWU. First, the physical model of some isolation wards in Huoshenshan Hospital is constructed, as shown in Figure 13 (a). In the design drawing of Huoshenshan Hospital, the starting point of disinfection robots is located in the nurse station in the center of the isolation ward. In the picture, the gray column in the center of the isolation ward is the charging station, and the four cyan squares are the disinfection robots. The whole simulation model includes 16 wards, which are located in the four corners of the map. The walls are used to isolate the wards. As shown in Figure 13 (b), The physical model of the isolation area of RHWU is irregular the other data are the same as Huoshenshan Hospital.

Experiment I: This experiment verifies the path planning and tracking without dynamic obstacles. It is assumed that the remaining power of four disinfection robots is 40Ah.

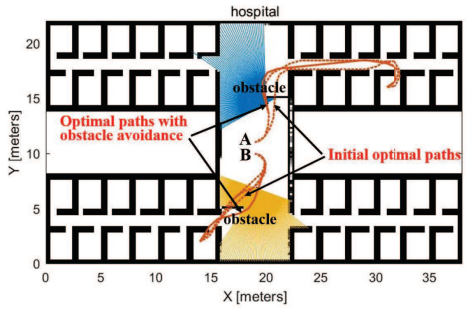

(a) Obstacle avoidance paths of two disinfection robots planned by A* algorithm first time.

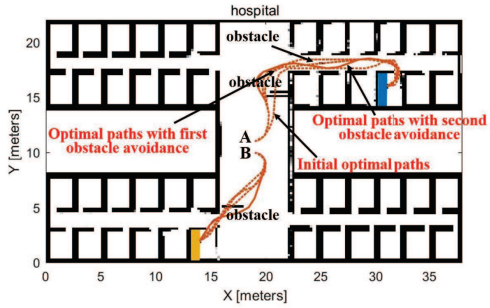

(b) Obstacle avoidance paths of two disinfection robots planned by A* algorithm second times.

Figure 12. Obstacle avoidance paths planned by A* algorithm.

(a) Physical model of Huoshenshan Hospital.

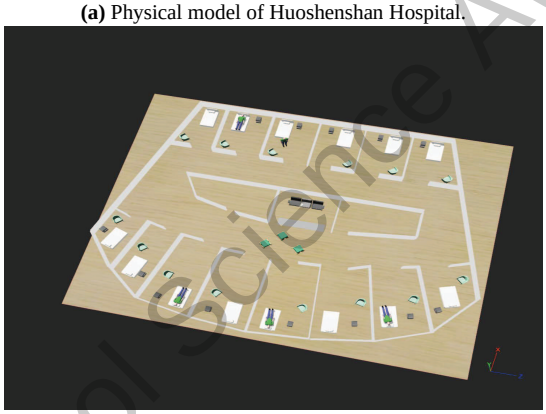

(b) Physical model of RHWU.

Figure 13. Physical model of hospital isolation area.

Figure 14 shows the disinfection path from the starting point to the target ward of four robots planned by A* algorithm. It can be seen from the figure that the robot can complete the disinfection tasks of the assigned wards in sequence according to the prescheduling, and the motion trajectories of different robots are represented by different colors.

Experiment II: Supposing that a dynamic obstacle appears in the environment, by using the same parameters as in Experiment I of Subsection 5.3, the dynamic obstacle avoidance of disinfection robots are achieved by using A*-DWA, as shown in Figure 15. It can be seen from the Figure 15 (b) that when dynamic obstacles (two persons) appear, the disinfection robot can use its own laser sensor to detect obstacles and hence complete dynamic obstacle avoidance.

6 Conclusion

Through analyzing the actual data from several hospitals during the period of COVID-19, this paper has distilled general criteria and operation requirements for the disinfection in isolation areas. Facing the cooperative disinfection task of multiple robots in large and complex environment, and combining the requirements of the related national standards, a strategy of multi-constraint optimal scheduling has been proposed based on VRP model under the constraints on remaining powers, disinfection tasks in key areas and starting positions. Then, the optimal scheduling of multiple disinfection robots has been achieved under different task requirements. Besides, recognizing the particularity of the isolation area environment, a novel A*-DWA algorithm of multiple disinfection robots path planing has been presented, to achieve global path planning in the known environment and local real-time dynamic obstacle avoidance in the unknown environment.

With the proposed model and algorithm, simulation experiments have been carried out based on the actual map data of Huoshenshan Hospital and RHWU. By MATLAB, the simulation experiments on global path planning via A* algorithm and RRT have been performed, which demonstrates that the optimal path planned by the former is smoother than the latter. The simulation experiment on dynamic obstacle avoidance merely via A* algorithm has also been performed, which exhibits that A* algorithm can achieve dynamic obstacle avoidance, but requires multiple path planning so as to result in the increasing of computation load. By combining Webots and Python, the A*-DWA of dynamic obstacle avoidance has been testified, which shows that the algorithm can well achieve path planning and obstacle avoidance in dynamic environment. By integrating the multi-constraint optimization scheduling model with A*-DWA, the dynamic scheduling and finite-time path planning problem of the multiple cooperative disinfection robots in large and complex environment is effectively solved, which provides effective theoretical basis and technical support for the equipment de-

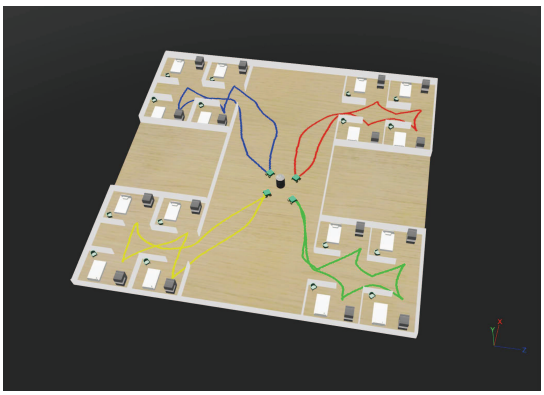

(a) Paths of robots for the disinfection of Huoshenshan Hospital.

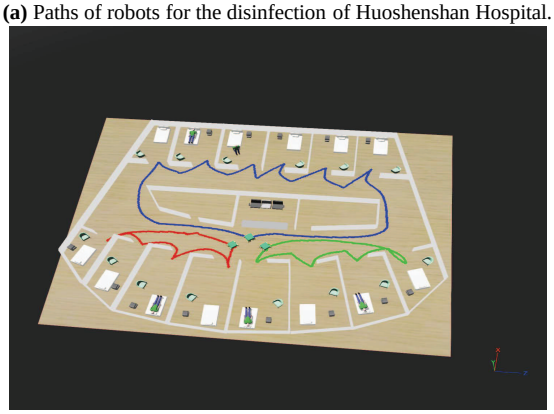

(b) Paths of robots for the disinfection of RHWU.

Figure 14. Paths of robots for disinfection task.

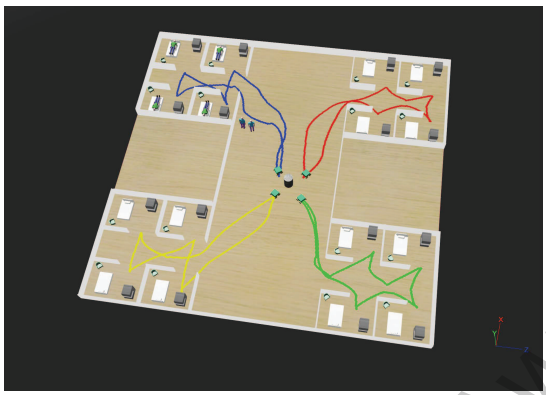

(a) Dynamic obstacle avoidance based on A*-DWA.

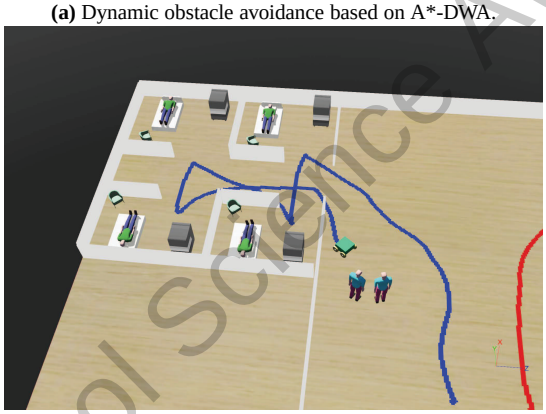

(b) Dynamic obstacle avoidance local enlarged drawing.

Figure 15. Dynamic obstacle avoidance paths planned by A*-DWA.

ployment and task scheduling of unmanned disinfection in hospitals.

Accordingly, by simulation, the optimal scheduling of multiple robots has been accomplished under three different conditions, and global path planning and dynamic real-time path planning and tracking of disinfection robots are achieved based on the actual map data of two isolation areas. These verify the feasibility and effectiveness of the proposed control method.

References

[1] Real Time Update: Corona Virus Disease 2019 Map [OL]. https://voice.baidu.com/act/newpneumonia/newpneumonia/?from=osari_aladin_banner #tab4. 2021.8.19.

[2] Jiang F, Yan Q M. A Summary of Essays on “the Impact of the COVID-19 Pandemic on China’s Economy” by Scholars of Department of Economics, Peking University[J]. Economic Science, 2020，2: 130-136.

[3] Huang Z X, Ma L, Liu T Y, Zhang H Y. Impact of Novel Coronavirus Pneumonia on World Economy and Politics[J]. Industrial Innovation, 2020(7): 34-36.

[4] Qiu D X, Zhang L C. Development of Medical Robots from the Perspective of Medical Staff Infection [J]. Hospital and Medicine, 2020, 1: 1-4.

[5] Human rights organizations: Mexico ranks first in the world in terms of new death toll of medical staff, the second in the United States, the United States, India and Brazil_Sina Technology_Sina.com[OL]. https://tech.sina.com.cn/roll/2020-09-04/doc-iivhuipp2489030.shtml. 2020.9.4.

[6] Xu B L, Guan J L, Shu C, et al. Advance in research on novel coronavirus[J]. Chinese Journal of Nosocomiology, 2020, 30(6): 839-844.

[7] Ding Z H, Hu G K. Application of Intelligent Robot in Hospital Disinfection[J]. Medical Information, 2020, 33(5): 28-29.

[8] Dong C R, Guo X, Li N, et al. Multi-robot dynamic path planning based on improved A* algorithms[J], Chinese High Technology Letters, 2020, 30(1): 71-81.

[9] Wang T T. Multi-Mobile Robot Path Planning Research[D]. Master Dissertation, Xi’an: Xi’an University of Technology, 2019.

[10] Yao C, Gao X L, Wu H Y, et al. Evaluation of disinfection effect of intelligent disinfection robot in operation room for patients with COVID-19[J], China Medical Equipment, 2020, 17(6):174-176.

[11] China National Evaluation Center for Robot Evaluation. ”Iron and Steel Soldiers” Fighting in the Front Line of Anti Epidemic[J]. Robot Industry, 2020, 2：90-109.

[12] Wang Y F. Application of Medical Robot in Major Epidemic Situation[J]. Sci-Tech & Development of Enterprise, 2020, 4: 62-64.

[13] Cheng J, Yang X, Chen J Y. Novel Coronavirus Pneumonia Isolation Ward for Nursing Care of Intelligent Disinfection Robot[J]. Science and Technology & Innovation, 2020, 13: 28-31.

[14] Shatalov M, Lunev A, Hu X, Sun W, Jain R, Yang J, Dobrinsky A, Deng J, Bilenko Yu, Moe C G, Wraback M, Shur M and Gaska R. Efficient UV emitters for sensing and disinfection[C].

In: Proceedings of Conference on Lasers and Electro Optics, San Jose, California, United States OSA, 2012: JTh1L.4.
[15] Mathebula T, Leuschner F W, Chowdhury S P. The use of UVC-LEDs for the disinfection of mycobacterium tuberculosis[J]. In: Proceedings of IEEE PES/IAS Power Africa, 2018, 739-744.
[16] Yang G Z, Nelson B J, Murphy R R, et al. Combating COVID-19—the role of robotics in managing public health and infectious diseases. Science Robot, 2020, 5: eabb5589.
[17] Chanprakon P, Saeoung T, Treebupachatsakul T, Hannantaanan P, Piyawattanametha W. An ultra-violet sterilization robot for disinfection[C]. In: Proceedings of the 5th International Conference on Engineering, Applied Sciences and Technology (ICEAST), 2019.
[18] Liu Y J. At Present, Titanium Rice Robots Reinforce the Front Line[J]. Robot Industry, 2020, 2: 60-63.
[19] Zhang H, Wang Y N, Yi J F, et al. Research on intelligent robot systems for emergency prevention and control of major pandemics[J]. Scientia Sinica (Informationis), 2020, 50(7): 1069-1090.
[20] Sina.com. Professor Hang Dian Develops Sterilization Robot to Assist Wuhan to Greatly Improve the Killing Speed of CT Detection Room[J]. Evaluation & Management, 2020, 18(1): 59.
[21] Gao F. Research on Distribution Routing Optimization Problems with Uncertain Factor[D]. Doctoral Dissertation, Beijing: Beijing Jiaotong University, 2019.
[22] CAI G Y, DONG E Q.Comparison and analysis of generation algorithm and ant colony optimization on TSP.Computer Engineering and Applications, 2007, 43(10) : 96-98.
[23] Chen X Y, Zhang D Y, Su X B, Dai Y H and Zhao C D. Cargo location optimization strategy based on improved genetic algorithm and multi-objective decision [J].Journal of Tianjin University of Science & Technology, 2020, 35(4): 317-333..
[24] Zheng Y B, Qiu X Y, Sun Y Y, et al. Research on Cold Chain Logistics Distribution Route Optimization Based on Genetic Algorithm[J]. Highways & Automotive Applications, 2020, 3: 49-52.
[25] Li J, Xie B L, Guo H H. Genetic Algorithm for Vehicle Scheduling Problem with Non-Full Load[J]. Journal of Systems & Management, 2000, 9(3): 235-239.
[26] Sun H C and Zhu Y H, Study on path planning for UAV based on probabilistic roadmap method [J].Journal of System Simulation, 2006, 18(11):3050-3054.
[27] Leng Z, Dong M Z, Dong G Q, et al. A rapid path planner for autonomous ground vehicle using section collision detection[J]. Journal of Shanghai Jiaotong University (Science), 2009, 14(3):306-309.
[28] Cao S M. Path planning algorithms of mobile robot in dynamic environment [D]. Doctoral Dissertation, Harbin: Harbin Institute of Technology, 2019.
[29] Wang D J, Indoor mobile-robot path planning based on a improved A* algorithm [J].Journal of Tsinghua University (Sci & Tech), 2012(8):1085-1089.
[30] Xu X Q, Wang M Y, Mao Y. Path planning of mobile robot based on improved artificial potential field method [J/OL]. Journal of Computer Applications: 1-5 [2020-09-02]. http://kns.cnki.net/kcms/detail/51.1307.TP.20200731.0944.002.html
[31] Ren G C, Hu X L, Liu P. Dynamic window approach for trailer mobile robot based on path tracking [J/OL]. Application Research of Computers:1-5 [2020-09-02]. https://doi.org/10.19734/j.issn.1001-3695.2019.09.0577.
[32] Guo N, Li C H, Wang D, Zhang N, Song L. Local path planning of mobile robot based on fuzzy control [J].Journal of Shandong University of Technology (Natural Science Edition),2020, 34(04): 24-29.
[33] Wang T. Research on obstacle avoidance of wheeled mobile robot based on wavelet neural network and fuzzy sliding mode control [J].Chinese Journal of Construction Machinery, 2020, 18(03): 278-282.